Utah State University

DigitalCommons@USU

All Graduate Theses and Dissertations, Fall 2023 to Present

Graduate Studies

12-2023

Fire and Flow: Assessing the Long-Term Effects of Wildfires and Impact of High Flow Events on Phosphorus Concentrations in Mountain Streams

Rachel Watts
Utah State University, rachel.watts@usu.edu

Follow this and additional works at: https://digitalcommons.usu.edu/etd2023

 Part of the Water Resource Management Commons

Recommended Citation

Watts, Rachel, "Fire and Flow: Assessing the Long-Term Effects of Wildfires and Impact of High Flow Events on Phosphorus Concentrations in Mountain Streams" (2023). *All Graduate Theses and Dissertations, Fall 2023 to Present*. 48.
https://digitalcommons.usu.edu/etd2023/48

This Thesis is brought to you for free and open access by the Graduate Studies at DigitalCommons@USU. It has been accepted for inclusion in All Graduate Theses and Dissertations, Fall 2023 to Present by an authorized administrator of DigitalCommons@USU. For more information, please contact digitalcommons@usu.edu.

UtahStateUniversity
MERRILL-CAZIER LIBRARY

FIRE AND FLOW: ASSESSING THE LONG-TERM EFFECTS OF WILDFIRES AND IMPACT OF HIGH FLOW EVENTS ON PHOSPHORUS CONCENTRATIONS IN MOUNTAIN STREAMS

by

Rachel Watts

A thesis submitted in partial fulfillment

of the requirements for the degree

of

MASTER OF SCIENCE

in

Watershed Science

Approved:

_____	_____
Janice Brahney, Ph.D. Major Professor	Benjamin Abbott, Ph.D. Committee Member
_____	_____
Erin Rivers, Ph.D. Committee Member	D. Richard Cutler, Ph.D. Vice Provost of Graduate Studies

UTAH STATE UNIVERSITY
Logan, Utah

2023

Copyright © Rachel Watts 2023

All Rights Reserved

ABSTRACT

Fire and Flow: Assessing the Long-Term Effects of Wildfires

And Impact of High Flow Events on Phosphorus

Concentrations in Mountain Streams

by

Rachel Watts, Master of Science

Utah State University, 2023

Major Professor: Dr. Janice Brahney
Department: Watershed Sciences

Although Phosphorus (P) is a key limiting nutrient in watersheds, important questions remain about its form, transport, and bioavailability in rivers, particularly during high flow events and after wildfire occurrence. Recent changes in weather patterns caused by climate change have led to longer, more intense droughts, irregular but high intensity storms, and more severe wildfires with longer burn durations. The combination of these environmental factors can affect a watershed's overall P mobility. The purpose of this study was twofold: 1. To investigate the long-term impacts of wildfires on P, and 2. To understand how high flow events affect P hysteresis patterns in streams. For one snowmelt season and two monsoon seasons, we collected water samples during 3 riverbed-disturbing, high flow events. We also evaluated the potential for riverbed sediment to contribute bioavailable P to the water column through laboratory experiments. We found that antecedent conditions of a riverbed and its respective watershed strongly influence P mobility during high flow events by controlling armoring

of streambed and soils, which influences whether P comes from proximal or distal sources. There was significant variation in streambed sediment P dynamics, with sediments acting as either a P source or sink between monsoonal years. To investigate the long-term effects of wildfire, we deployed P binding devices in 8 streams located within a 9-year-old burn scar in low to moderately burned areas. Despite short-term spikes in stream P concentrations typically observed after a fire, long-term P abundance was lower in burned than unburned watersheds. We found that watersheds with low-moderate burn severity had significantly lower P concentrations ($p=0.01$) when compared to control watersheds, with an average decrease of 62%. Unchanged-Low severity burn sites decreased by 10% when compared to Unburned watersheds ($p=0.66$) and increased by 52% relative to Low-Moderately burned sites ($p=0.04$). Additionally, outside of variations in burn severity, the watershed parameters most correlated with P abundance in streams were soil permeability ($r=0.92$, $p=0.00$) and vegetation type ($r=0.80$, $p=0.02$), suggesting decreases are a combination of post-fire landscape modifications including decreased soil permeability and environmental succession.

(86 pages)

PUBLIC ABSTRACT

Fire and Flow: Assessing the Long-Term Effects of Wildfires and Impact of High Flow Events on Phosphorus Concentrations in Mountain Streams

Rachel Watts

Climate change has led to significant shifts in the Earth's weather patterns, often leading to longer, more intense droughts, irregular but extreme storms, and more severe wildfires with longer burn durations. These weather pattern changes have frequently led to shifts in ecosystem dynamics, impacting aspects such as nutrient flux, species diversity, and overall habitat health. Regarding nutrient flux specifically, changes in phosphorus (P) concentrations can negatively impact stream systems as elevated levels can lead to toxic algal blooms, which can cause habitat degradation, loss of usable recreational areas, and large fish kills. A common trigger of these P spikes is the occurrence of wildfires. As fire burns plants and other organic matter, it can often release trapped P, making it available for uptake by flora and fauna. However, if it is not immediately taken up, it can be transported to streams via storm runoff. Furthermore, as droughts, another common trigger, continue to get more severe, the likelihood of P accumulation throughout undisturbed water pathways and riverbed sediments significantly increases. Then, once a storm finally occurs and the flow pathways are disturbed, the accumulated P is mobilized and transported to streams via runoff, further contributing to spikes in P levels. In this study, we explored the influence of riverbed disturbance on stream P concentrations as well as the potential existence of any long-term

repercussions of wildfire on P mobility. For one spring snowmelt season and two summer monsoon seasons, we collected water samples during riverbed-disturbing high flow events and deployed P catching devices in streams located in a 9-year-old burn scar. We found that riverbed sediments disturbed by high intensity rainstorms can influence the overall source of P in water columns, which switched between proximal and distal sources. We also found that despite short-term spikes typically found after a wildfire, stream P levels can significantly decrease long-term. This knowledge is important because a better understanding of these trends could foster improvements of strategies for water quality monitoring, restoration efforts, and the protection of natural resources by managing agencies.

ACKNOWLEDGMENTS

To my advisor, Dr. Janice Brahney, thank you for all the time and energy you put into helping me with this project and for guiding me through all the bumps in the road associated with this project. I am so grateful that I got to work with someone so brilliant and creative in the scientific field. I would not have made it through this project without your constant support and advocacy. I appreciate everything you have done for me as well as the encouragement you have shown me over the past 2.5 years. Thank you to Dr. Erin Rivers for all your help with math and statistics. I am so glad that I got to know you through this project.

To the Labbott Supreme Leader, Dr. Ben Abbott, thank you for steering me towards this program and always giving me a loving and supporting shoulder to lean on when times were tough. I could not have made it through my undergraduate and graduate experiences without you. I feel honored to call you an advisor, colleague, and friend. Your constant kindness, optimism, and encouragement over the past 6 years is something that I will always appreciate and cherish. I recognize that you have opened countless doors for me and have always cheered me on.

To Nicole Hucke, thank you for being my Ph.D. counterpart on this project. You have become my best friend and I will always cherish all the of memories we made during this project. You have always been so supportive and encouraging from day one and I am beyond grateful that we got to work on this project together. You are so smart, innovative, kind, and funny and I loved getting to know you. You are a rock star.

To my lab mates and cohort friends, Elana Feldman, Diane Wagner, Macy Gustavus, Molly Blakowski, Gordon Gianniny, Mark Devey, Audree Provard, Jiahao Wen, Jaunma Gonzales-Olalla, and Camilla Moses, thank you for all your support, troubleshooting ideas, and fun conversations. I am so glad that I got to know all of you during this process and I recognize all the help you all have given me during my time here. A massive thank you, as well, to the Los Alamos National Laboratory team, George Perkins, Rose Janina, and Joel Rowland, for all your help and guidance both in the field and lab while Nicole and I were working in New Mexico.

Last but not least, a huge and loving thank you to my family- Dad, Mom, Nathan, Katherine, Jennifer, and Kacen. Thank you for all the support, solidarity, and patience you have given during this project. I love you all so much and you mean the world to me. Dad- I dedicate this thesis to you. Thank you for always being such a brilliant, scientific thinker and for pushing me to always do my best. You have shown me what it means to be a steward of the Earth and how to appreciate everything that Mother Nature has to offer. You fostered my love for nature, and I couldn't be more grateful.

Rachel Watts

CONTENTS

Page

LIST OF TABLES

Page

LIST OF FIGURES

Page

CHAPTER 1: GENERAL INTRODUCTION

Phosphorus (P) is a key limiting nutrient in watershed systems, influencing production, species composition, and habitat conditions (Chow et al., 2017; Yan et al., 2019; House, 2003; Zhou et al., 2005; Lapworth et al., 2011). Yet, important questions remain on the form, transport, and bioavailability of phosphorus compounds in river systems, particularly during high flow events and a decade after wildfire occurrence (Atkinson et al., 2019). When high flow events from storm activity or snowmelt occur, they have the potential to mobilize phosphorus from the catchment and/or sediments into the water column (Ross et al., 2019; Kerr et al., 2011), affecting overall stream P concentrations. As such, it is uncertain how armor layer conditions and riverbed composition interact to influence the mobilization of streambed resources and the bioavailability of P in streams during high flow events. Watersheds affected by wildfires often undergo changes in ecological properties that result in changes in nutrient flux and transport (Xue et al., 2014; Johnson et al., 2012). These wildfire effects can also significantly increase the likelihood of P mobilization in watersheds as P-rich ash and other particulates are transported to streams by storm runoff and leaching (Son et al., 2015; Qian et al., 2009). Therefore, the purpose of these studies is to investigate the long-term impacts of wildfires and understand how high flow events affect overall P concentrations in streams and how they may be expected to change in the future. Knowledge of these impacts could foster better strategies for water quality monitoring, restoration efforts, and the protection of natural resources by managing agencies.

REFERENCES

Atkinson, C. L., van Ee, B.,C., Lu, Y., & Zhong, W. (2019). Wetland floodplain flux: Temporal and spatial availability of organic matter and dissolved nutrients in an unmodified river. *Biogeochemistry, 142*(3), 395-411. doi:https://doi.org/10.1007/s10533-019-00542-z

Chow, M. F., Huang, J., & Shiah, F. (2017). Phosphorus dynamics along river continuum during typhoon storm events. *Water, 9*(7). doi:https://doi.org/10.3390/w9070537

House, W. A. (2003). Geochemical cycling of phosphorus in rivers. *Applied Geochemistry, 18*(5), 739-748. Retrieved from https://login.dist.lib.usu.edu/login?url=https://www-proquest-com.dist.lib.usu.edu/docview/19813174?accountid=14761

Johnson, D. W., Walker, R. F., McNulty, M., Rau, B. M., & Miller, W. W. (2012). The long-term effects of wildfire and post-fire vegetation on sierra nevada forest soils. *Forests, 3*(2), 398-416. doi:https://doi.org/10.3390/f3020398

Kerr, J. G., Burford, M. A., Olley, J. M., Bunn, S. E., & Udy, J. (2011). Examining the link between terrestrial and aquatic phosphorus speciation in a subtropical catchment: The role of selective erosion and transport of fine sediments during storm events. *Water Research, 45*(11), 3331-3340. doi:https://doi.org/10.1016/j.watres.2011.03.048

Lapworth, D. J., Gooddy, D. C., & Jarvie, H. P. (2011). Understanding phosphorus mobility and bioavailability in the hyporheic zone of a chalk stream. *Water, Air and Soil Pollution, 218*(1-4), 213-226. doi:https://doi.org/10.1007/s11270-010-0636-1

Qian, Y., Miao, S. L., Gu, B., & Li, Y. C. (2009). Estimation of postfire nutrient loss in the florida everglades. *Journal of Environmental Quality, 38*(5), 1812-20. Retrieved from https://login.dist.lib.usu.edu/login?url=https://www.proquest.com/scholarly-journals/estimation-postfire-nutrient-loss-florida/docview/347858217/se-2?accountid=14761

Ross, D. S., Wemple, B. C., Willson, L. J., Balling, C. M., Underwood, K. L., & Hamshaw, S. D. (2019). Impact of an extreme storm event on river corridor bank erosion and phosphorus mobilization in a mountainous watershed in the northeastern united states. *Journal of Geophysical Research.Biogeosciences, 124*(1), 18-32. doi:https://doi.org/10.1029/2018JG004497

Son, J., Kim, S., & Carlson, K. H. (2015). Effects of wildfire on river water quality and riverbed sediment phosphorus. *Water, Air and Soil Pollution, 226*(3), 1-13. doi:https://doi.org/10.1007/s11270-014-2269-2

Xue, L., Li, Q., & Chen, H. (2014). Effects of a wildfire on selected physical, chemical and biochemical soil properties in a pinus massoniana forest in south china. *Forests, 5*(12), 2947-2966. doi:https://doi.org/10.3390/f5122947

Yan, W., Liu, L., Wu, T., Song, L., Wang, H., Lu, Z. Zhu, Y. (2019). Effects of short-term aerobic conditions on phosphorus mobility in sediments. *Journal of Freshwater Ecology, 34*(1), 649-661. doi:https://doi.org/10.1080/02705060.2019.1659190

Zhou, A., Tang, H., & Wang, D. (2005). Phosphorus adsorption on natural sediments: Modeling and effects of pH and sediment composition. *Water Research, 39*(7), 1245–1254. doi:https://doi.org/10.1016/j.watres.2005.01.026

CHAPTER 2: EFFECT OF HIGH FLOW EVENTS ON PHOSPHORUS MOBILITY IN STREAMS

1. INTRODUCTION

Phosphorus (P) is a key limiting nutrient in watershed systems, influencing production, species composition, and habitat conditions (Chow et al., 2017; Yan et al., 2019; House, 2003; Zhou et al., 2005; Lapworth et al., 2011). Yet, important questions remain about the form, transport, and bioavailability of P compounds in river systems, particularly during high flow events (Atkinson et al., 2019). High flow events from storm activity or snowmelt can mobilize P from the catchment soils and stream network sediments into the water column (Ross et al., 2019; Kerr et al., 2011), which can impact algal production and therefore water quality (Vidon et al., 2011; Lapworth et al., 2011; Frazar et al., 2019). However, it is uncertain how riverbed armor layer conditions and sediment composition interact to influence the mobilization of streambed nutrient resources and the bioavailability of P in streams during high flow events.

Climate change is expected to increase the intensity of the hydrologic cycle and, as such, the frequency and intensity of storms will become more variable (Bruine de Bruin Wandi et al., 2022; IPCC, 2014; File et al., 2020; Zhou et al., 2018). As storm water flows through a river, its hydrologic force, or shear stress, can cause sediments on the riverbed to mobilize once the critical shear stress is reached (Correll et al., 1999; Chow et al., 2017). Upon reaching the critical shear stress, heavier material- such as cobbles, pebbles and rocks (otherwise known as the ‘armor layer’) can be moved by the water, exposing and disturbing the sediments underneath (Anju et al., 2020). High

intensity storms have the potential to increase the rate of P mobilization as larger amounts of runoff increase a river's shear stress, promoting more substantial armor layer disturbance.

As these fine sediments are disturbed by armor movement, they can become entrained by the water column and undergo redox and/or equilibrium reactions that either sorb or release P to or from the water column. This movement of P can lead to fluctuations in overall stream concentrations of either or both particulate P (PP) or soluble reactive (SRP) as these fractions move through the various stages of nutrient spiraling. The nutrient spiraling process, which describes the cycling of nutrients through aquatic systems, consists of several stages: uptake/release through flora and fauna, transformation via chemical reactions, transport through watersheds, and settling of particles onto the riverbed either within or on top of the armor layer (Webster, 1975; Ensign & Doyle, 2006; Finkler et al., 2021). P and other nutrients can transition through any of these stages at any point during the spiraling process as mobility is affected by environmental factors such as rainfall, wildfires and other disturbance events (Yan et al., 2019, 2020; Buckingham et al., 2010; He et al., 2018; Correll et al., 1999). Nutrients mobilized from more distal groundwater sources will be in dissolved form while landscape erosion can contribute PP and SRP to the river through similar mechanisms described above. The source of P in the water influences the concentrations of particulate phosphorus (PP) and soluble reactive phosphorus (SRP) in the river system (Bowes et al., 2005; Jarvie et al., 2006), and the form of P influences its bioavailability (Frazar et al., 2019; He et al., 2018). As such, the bioavailability of the mobilized P can vary by whether the P is sourced from either a distal zone (i.e., transported via runoff) or

proximal zone (i.e., sediments from within the riverbed) (Frazar et al., 2019; Anju et al., 2020), as well as the composition of riverbed sediments.

The composition of riverbed sediments will dictate whether sediments will sorb or release SRP once entrained in the water column. Sediment grain size as well as the concentration and form of nutrients will influence how P is released in the water column, and thus its bioavailability to primary producers and other microbiota in the water column (Vidon et al., 2011; Lapworth et al., 2011; Frazar et al., 2019). Fine sediments are typically more organic and clay-rich (Lottig et al., 2007; Stone et al., 2004; Lapworth et al., 2011). As a consequence, they are typically richer in both particulate and exchangeable P (Stone et al., 2004; Buckingham et al., 2010).

In addition, other constituents such as Calcite, Fe/Mn and Al oxides can tightly bind and or release P under different pH and redox conditions (He et al., 2018; Chen et al., 2015). Whether the sediments will act as a source or a sink can be determined by testing the sediments' equilibrium point concentration (EPC_o) prior to mobilization. The sediments' EPC_o is determined through successive nutrient addition experiments to derive the point at which no net release or uptake of SRP occurs (when the rates of desorption and adsorption are the same (Pierzynski et al., 1994), meaning that as the EPC_o of a riverbed's sediment changes, the response of SRP in the water column can differ (Lottig et al., 2007).

Determining hysteresis patterns during high flow events will provide information on the source and bioavailability of P during high flow events as well as how streambed mobilization impacts SRP and PP. Hysteresis patterns can tell us if the majority of P is

coming from a proximal or distal source (Chen et al., 2013; Bowes et al., 2005). These patterns are affected by changes in the rate at which water flows through a watershed, influencing nutrient spiraling activity as sediments and associated P are mobilized and transported (Frazar et al., 2019; Ensign et al., 2005). As a high flow event mobilizes PP or SRP near or in the river, the concentration of P in the water will be highest on the rising limb of the hydrograph. This is because the distance traveled by P from the proximal source to the river is shorter, allowing the P to reach the river quickly (Chen et al., 2013; Bowes et al., 2005). If the PP or SRP in the water column is coming from a distal source in the upper highlands, then the pattern will be a smaller, counterclockwise loop, and the concentration of P in the water will be highest on the falling limb of the hydrograph. This is because it takes a longer amount of time for the P to travel from the distal source to the river, delaying the peak concentration (Chen et al., 2013; Bowes et al., 2005; Chow et al., 2017). Thus, it is hypothesized that changes in P mobility from the disturbance of streambed armor will influence P hysteresis pattern directionality.

Our working hypotheses are, **HY_1- Armor-disturbing high flow events mobilize streambed particulate and dissolved phosphorus**. **HY_2- Fine sediment-P composition influences water column P bioavailability and resulting hysteresis patterns during high flow events.** Here, we tested these hypotheses through river monitoring and in situ river manipulations in New Mexico's Jemez watershed. Water samples with suspended sediments mobilized during high flow events will be analyzed for TP, SRP, and PP to evaluate the potential implications to the ecosystem. Sediment cores will be taken during normal flow conditions and will be analyzed for EPC_o in addition to TP, SRP and PP.

2. METHODS

2.1 Study Area

Jemez watershed (Figure x) is a pristine environment that will allow for an accurate depiction of P mobility along two reaches La Jara Creek (marked by the red star) as related to high flow storm and snow melt events. This stream originates from the Valles Caldera. La Jara Creek drains a 3.7 km^2 area of 26% evergreen forests, 52% grassland, and 18% shrubland (New Mexico Environment Department, 2006; USGS Stream Stats) and is located within the Valles Caldera National Preserve (VCNP). This Caldera is about 15 km northeast of Jemez Springs and 30 km west of Los Alamos in the northern volcanic Jemez Mountains of northern New Mexico (Liu et al., 2008). The Jemez Mountains are in the transition zone between the snow-dominated Rocky

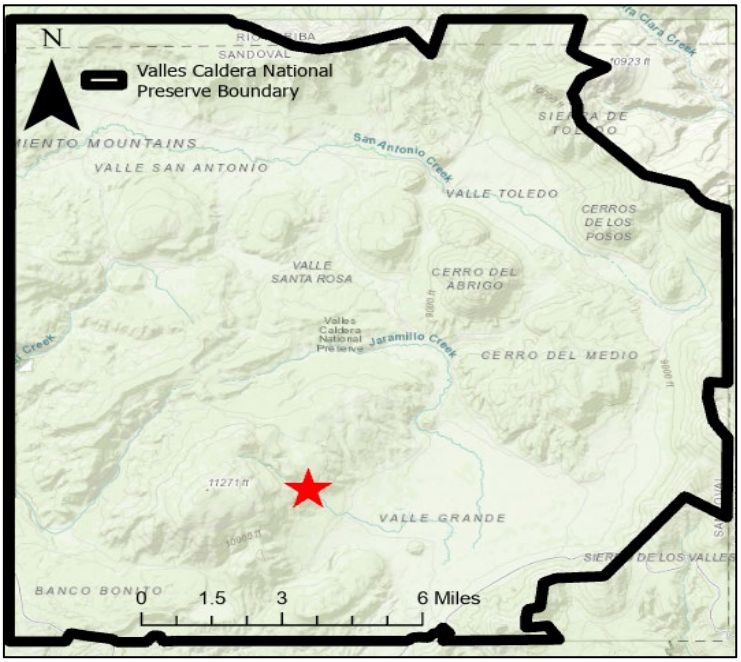

Figure 1.1: Location of La Jara Creek (red star) in the Valles Caldera National Preserve, New Mexico, USA.

Mountains and the monsoon-dominated southwestern United States, resulting in a bimodal pattern of annual precipitation (Brooks et al., 2008; Perdrial et al., 2013).

Elevations range from 2300 m at Redondo Meadow to 3432 m at Redondo Peak. Since the early 1980s, the annual temperature has averaged 9 °C and precipitation averaged 476 mm, as measured in a neighboring site at an elevation of about 2200 m in Los Alamos (Liu et al., 2008; Bowen et al., 1996; Perdrial et al., 2013). Mean precipitation from October to April accounts for 40% of the annual total and falls primarily as snow (Gustafson et al., 2010; Rinehart et al., 2008). Mean precipitation during the monsoon season in July and August represents approximately 50% of the annual precipitation (Liu et al., 2008; Bowen et al., 1996; Sherson et al., 2015). This precipitation regime will allow us to test our **HY_1** - that changes in shear stress of the water column will influence the movement of sediments after river armor disturbance, impacting P mobility in the water column. Stream discharge typically peaks in late March to early April corresponding to spring snowmelt, and a gradual recession lasts until the onset of the following spring's snowmelt. Summer monsoon precipitation events in July through September occasionally lead to sporadic increases in stream discharge, but these are minimal compared to the snowmelt pulse, as much of the summer precipitation returns to the atmosphere via evapotranspiration (Broxton et al., 2009; Liu et al., 2008; Zapata-Rios et al., 2015; McIntosh et al., 2017). The riverbed is armored with cobbles and gravel. Underlying deposits consist of very poorly sorted, unconsolidated volcaniclastic and colluvial sediment ranging from silt to boulders (Sawyer et al., 2012).

La Jara Creek was chosen because the watershed has previous measurements and information that were useful to the project such as Q and nutrient monitoring by the

USGS and CZO. This watershed also has snow melt activity in the spring and monsoon events in the summer, potentially allowing for multiple high flow events throughout sampling seasons. Gaining and losing reaches were documented by lead investigators using ADV measurements. One gaining and one losing reach were monitored and sampled for our study. Finally, the creek had a sufficient armor layer protecting a layer of fine sediment. This fine sediment had the potential to be disturbed during high flow events and possibly produce the hysteresis patterns we wanted to study.

2.2 Data Collection and Preservation

2.2.1 Storm water samples

We explored **HY_1** by collecting water samples during armor-moving storm events in real time using automated ISCO samplers. Field work was conducted over the course of the 2021 and 2022 monsoon seasons to ensure plenty of storms could be studied. Despite this redundancy plan, however, only three armor-moving storm events occurred, leaving us with limited replicates and data. PP and SRP were analyzed from select samples chosen using the storm's hydrograph obtained from deployed pressure transducers. We aimed to collect 5 samples per storm: 1-2 samples on the rising limb of the hydrograph, 1 at the peak, and two on the falling limb of the hydrograph. All samples were stored in a cooler until arrival at Los Alamos National Laboratory (LANL), where they were filtered with a 0.45 μm Glass Fiber Filter (GFF) or a Cellulose acetate filter (CAF) and stored in a freezer with minimal light exposure. Unfiltered samples were used for TP analysis. Filtered samples were used for SRP analysis. The 0.45 μm filter was stored in a refrigerator and used for PP analysis.

Q measurements were obtained using the CZO database for the 2021 field season. However, in 2022, rating curves made from pressure transducer datum had to be used to obtained Q measurements as the CZO monitoring equipment malfunctioned. While no water samples were obtained from the upper reach of La Jara due to instrument malfunction across both sampling seasons, we were able to obtain sufficient data from the lower reach. After all samples were analyzed for SRP, TP, and PP concentrations, the results were subsequently plotted against the storm's Q. The resulting pattern was determined to be either clockwise or counterclockwise, informing us of the primary source of P to the water column.

2.2.2 Dam Release Water Samples

We further explored **HY_1** by conducting a series of dam release experiments that artificially created an armor-moving pulse event. For these experiments, a section of La Jara Creek, downstream of our primary experimental sites, was chosen for its optimal location and stream characteristics as it had a relatively uninterrupted flow, tall stream banks that allowed water to build-up behind the dam (rather than simply flowing into the floodplain) and was heavily armored. The total reach was approximately 60 meters long, beginning just below a confluence in a heavily vegetated area.

A temporary dam was built using a 4x8 ft plywood sheet, three tarps, rocks from the riverbed, and approximately 45 sandbags. The plywood sheet was cut to fit the general shape of the channel. U-bolts were fastened to both sides of the sheet to serve as makeshift handles which allowed for easier removal of the dam. One tarp was used to line the bottom the riverbed and was weighed down by rocks. The remaining tarps were used to line the banks of the river to a) prevent any erosion due to our experiment and b)

prevent the addition of non-riverbed sediment to our experiment. This allowed us to essentially have an artificial seal that promoted better water retention by preventing water from flowing underground/into the stream banks, under/around the dam, and out the other side. The sandbags were used to plug any leaks surrounding the dam, further promoting optimal water retention for larger pulse events. These sandbags were filled with sandy loam, encased in heavy-duty trash bags, tied shut, and then sealed with duct tape. This helped to prevent water from seeping through the sandbags and potentially contaminating our samples with ex situ sediment.

Once the dam was secured in place, the water was allowed to back up until it made a pool approximately 65 cm deep. The dam was then quickly removed, releasing a large pulse of water and artificially creating a high-flow event. Throughout the first high-flow event, “upstream” and “downstream” samples were collected approximately 4 meters and 60 meters below the dam release site, respectively. To collect samples, a reach pole was fashioned out of a PVC pipe and heavy-duty wire. After 2 holes were drilled into one end of the PVC pipe, the wire was woven through the holes and molded into a basket-like shape to hold an ISCO sampling bottle. Upon release of the dam, the operator of the reach pole secured a pre-labeled, acid washed ISCO bottle in the basket and submerged the bottle into the flood until the bottle was full.

We conducted a total of 5 dam releases. Of these 5 pulse events, we aimed to determine how the results varied between the first and last experiment, specifically. These experiments will be referred to as: Experiment 1- Upstream: E1.U where samples were collected approximately every 10 seconds; Experiment 1- Downstream: E1.D where samples were collected approximately every 10 seconds; and Experiment 5- Upstream:

E5.U where samples were collected approximately every 5 seconds. All samples were filtered and stored in a freezer within 48 hours following the same methods as above and then analyzed for SRP, TP, and PP. Results were graphed and analyzed for hysteresis patterns.

2.2.3 Sediment Samples

We explored **HY_2** by extracting 38 small sediment cores from the upper and lower reaches of our study site and analyzing them for SRP, organic phosphorus (OP), TP and EPC_0. We collected these samples before the first storm of the season and after each subsequent storm with the aim of testing how the storms changed the P content in the riverbed. Sample collection was done using a 60 mL syringe with its luer lock and hub cut off. With the syringe's plunger fully depressed, the syringe head was placed on the riverbed's surface and twisted in a circular motion while being pushed into the riverbed. The plunger would rise out of the syringe barrel as it filled with sediment. The same process was conducted for each sample obtained. All samples were placed in whirl-Paks™ and stored in a refrigerator until analysis could be conducted.

Samples were taken throughout 3 field seasons. In summer 2021, 8 samples were taken from cross sections of the middle region of each reach on 7/16, 7/27, 8/5, and 8/13. In spring 2022, throughout the duration of snowmelt season, 18 samples were taken from cross-sections of the top, middle, and bottom areas of each reach on 3/13, 3/18, 4/1. Because we could not be certain if the differences amongst the summer values in P were from time alone, we decided to take samples throughout additional cross sections in both reaches, as well. In Summer 2022, 12 samples were taken from cross-sections of the top,

middle, and bottom areas of each reach on 7/12 and 8/4. These samples were analyzed for EPC_0 only.

2.3 Laboratory Analyses

2.3.1 Water Samples

All filtered and unfiltered water samples collected from storms and dam release experiments were analyzed for SRP and TP, respectively, using a version of the standard EPA molybdate blue method 365.3. PP analysis was conducted on the CA and GF filters that were freeze dried to remove any moisture from the sample. The filter was then weighed and ashed in a muffle furnace at 550 C for 4 hours. A solution of 1M HCl and DI water was added to the centrifuge tubes, which were then placed on a shaker table for 16 hours. A molybdate blue reagent was then added to the shaken samples and allowed to develop for 30 mins. All PP samples were then run on a SpectraMax M2e.

2.3.2 Sediment Samples

All sediment samples obtained during the summer 2022 and winter 2023 field seasons underwent a three-step sequential extraction process. All sediment samples were freeze dried and approximately 0.5 g of sediment was used to 50 mL of reagent. Step one of the sequential extraction process utilized 1M $MgCl_2$ to shaken with sediment for 30 minutes to extract loosely sorbed P measured as soluble P**.** The second extraction used 1M NaOH to determine organic P as the difference between the soluble reactive and oxidizable fraction that is leached. For this extraction, the sediment and reagent were shaken for 16 hours and then centrifuged at 3900xg for 10 minutes. Soluble P was measured using the molybdate blue method described above while oxidizable P was measured using the EPA method 365.3 for TP analyses. Total sediment P was determined

on a separate subsample where approximately 0.5 g of sediment was ashed at 550°C for 2 hours. P was then leached using 1M HCl and TP measured as above. All samples were run on a SpectraMax M2E spectrophotometer.

Summer 2021 and Spring 2022 samples used in the EPC_o analysis were taken from the middle of each reach on 7/16/21, 7/27/21, 3/13/22, 3/18/22, and 4/1/22. Summer 2022 samples were taken from the top of each reach of the stream on 7/12/22, and 8/4/22. The sediment samples were split into 10 subsamples, each weighing approximately 0.5 g. Using the procedure from Hongthanat et al (2010), 10 stock solutions were made using 0.01M $CaCl_2$ containing 0, 0.01, 0.05, 0.10, 0.25, 0.5, 0.75, 1, 5, 10 mg P·L-1 as KH_2PO_4. Using a soil to solution ratio of 1:25, sufficient stock solution was added to its corresponding subsample, shaken for 24 hours, and centrifuged for 10 mins at 3900xg. All samples were then added to a molybdate blue reagent in a 1:4 ratio and allowed to develop for 30 minutes. Samples were then analyzed for C (Eq. 1), the concentration of SRP after a 24 h equilibration (mg/kg), via spectrophotometer.

(Eq. 1) $$\frac{C}{S} = \frac{C}{S_{max}} + \frac{1}{kS_{max}}$$

C = concentration of P in solution after 24-hr equilibration (mg·L-1)

S = the amount of P sorbed on solid phase (mg/kg)

S_{max} = maximum P sorption capacity of soil (mg/kg)

k = a constant related to the bonding energy (L/mg)

Once C was obtained, the Linearized Langmuir Adsorption Equation was used to find S, the total amount of P retained by the solid phase (mg/kg) (Hongthanat et al., 2010). C (mg·L-1) was then plotted against S (mg/kg) and a linear regression (Eq. 2) was performed to find EPC_o, the point at which the line crossed the x-axis.

(Eq. 2) $$S = KC - S_o$$

S = P sorbed on solid phase (mg/kg)

C = P remaining in solution after 24 h equilibration (mg·L-1)

S_o = Initial quantity of sorbed soil P (mg/kg)

K = slope, P equilibrium buffering capacity (PEBC, L/kg)

The EPC_o was then compared the water columns SRP content to determine if the riverbed was a source or sink of P to/from the water column.

3. RESULTS

3.1 Storm water samples

Across both field seasons, we had three armor-moving storms in total. Storm 1 occurred 7/23/21 (Q≤ 3.79 cfs), with samples taken from ISCOs 2 and 3. Analyses of the precipitation data indicate this was the first armor-moving storm in over 30 days. ISCO 3 was triggered by the river flow about one hour earlier than ISCO 2, perhaps because the stream reaches a bottle neck in flow where ISCO 3's sensor is located, prompting the water level to rise more rapidly in that location. Storms 2-3 occurred in 2022 on 8/3 (Q≤ 2.95 cfs), and 8/8 (Q≤ 4.6 cfs), respectively. All obtained samples were from ISCO 3 only, as ISCO 2 was not triggered.

SRP (mg·L-1) results demonstrated a counterclockwise hysteresis pattern (Fig. 2) for the most intense storm that occurred (Q ≥ 4.6 cfs), and a clockwise pattern for the two

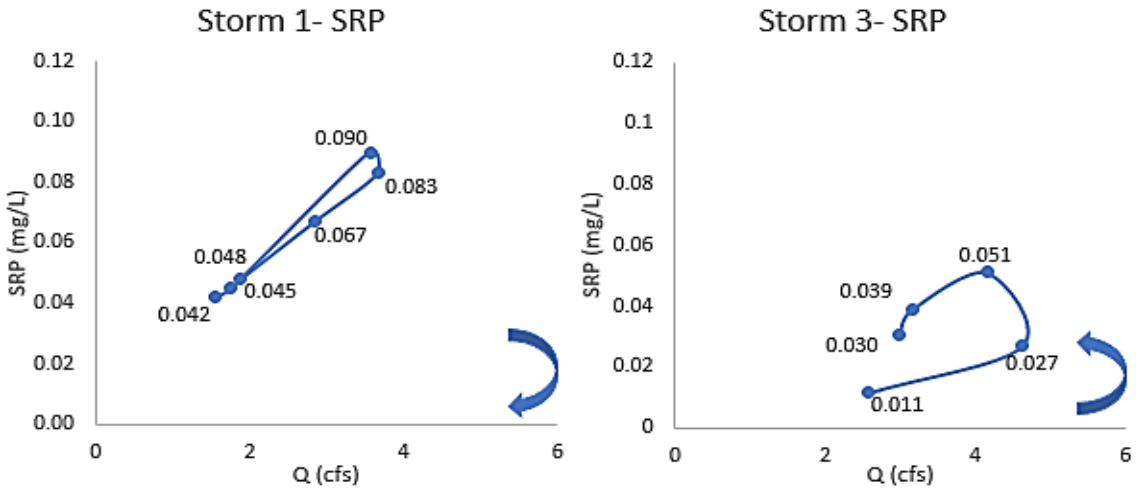

Figure 1.2: SRP (mg/L) hysteresis curves for Storm 1-ISCO 3 and Storm 3. Blue arrows depict directionality of the curve, which is clockwise for Storm 2 and counterclockwise for Storm 3. Blue dots indicate data points.

lower intensity storms (Q ≤ 3.79 cfs), suggesting there could be a threshold discharge that influences whether the dominant source of P is from the riverbed versus the catchment.. The counterclockwise hysteresis pattern in both TP and SRP from the largest storm suggests a distal primary SRP source. The less intense storms (Q≤ 3.79, Q≤ 2.95 cfs) were still capable of moving the armor layer and hysteresis patterns suggested a proximal primary SRP and TP source.

3.2 Dam Release water samples

While PP hysteresis patterns were consistently clockwise during the dam release experiments, changes in TP (PP+SRP) and SRP concentrations were minimal and resulted in a lack of distinguishable hysteresis patterns altogether, likely due to the

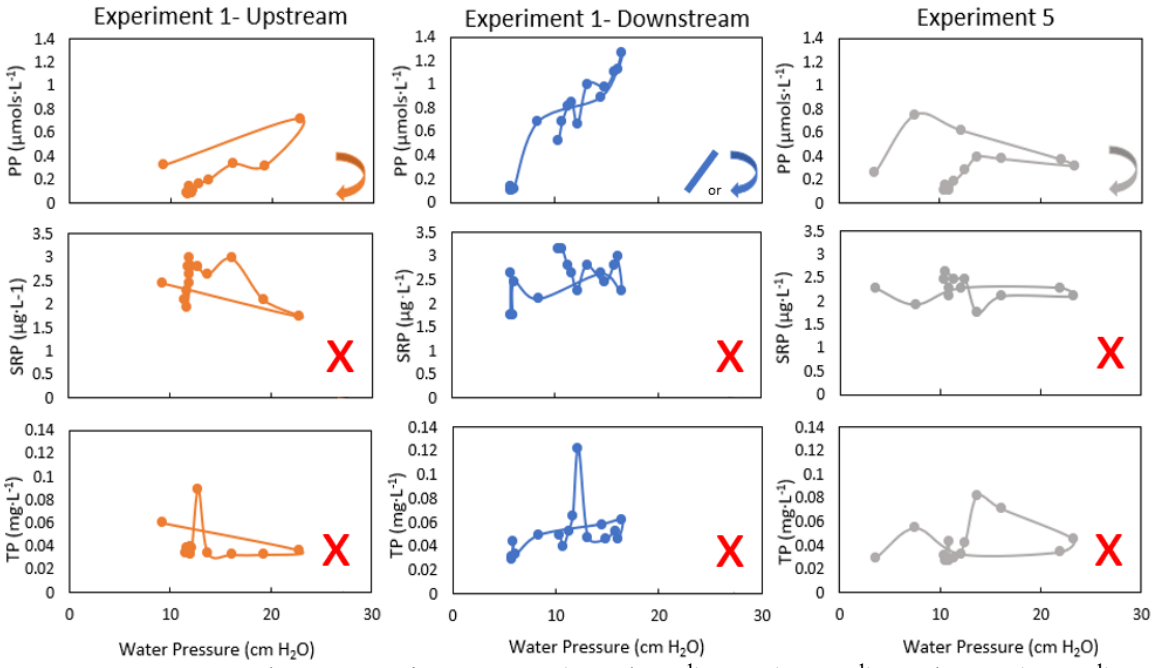

Figure 1.3: Dam release experiments' PP (µmols·L^{-1}), TP (mg·L^{-1}), and SRP (µg·L^{-1}) hysteresis curves. Arrows depict curve directionality, which is either clockwise or counterclockwise. A red "X" in place of arrows indicates the lack of a distinguishable hysteresis pattern. Orange data are for E1.U, Blue for E1.D, and Grey for E5.U.

limited exposure of the sediments to the water column. As expected, all PP hysteresis patterns were clockwise (Fig. 1.3), as there were no contributions to PP concentrations from overland flow. However, one could also interpret the samples taken during E1.D as a linear pattern, as well, with how tightly the hysteresis graph curves as PP concentrations rise, peak, and decrease with Q. As previously stated, TP and SRP concentrations had no distinguishable hysteresis patterns with overall ranges of 0.03-0.12 ($\mu g \cdot L^{-1}$) and 1.75-3.16 ($\mu g \cdot L^{-1}$), respectively, across all 3 experiments. The E1.D samples however, had slightly higher SRP concentrations at the end of the hydrograph when compared to the upstream samples.

3.3 Sediment Samples

There was no significant difference in sediment P between storms, reaches as a whole, or across time. An ANOVA was performed on samples from summer 2021 for all three P fractions (SRP, OP, and TP) to see if there was a statistical difference in P concentrations before and after an armor-moving storm event and between our upper and lower reaches. All P-values were shown to be insignificant. ANOVAs were also performed on the samples from Spring 2022, indicating that even though sediment P was highly variable across space and time, significant differences were unable to be detected as these changes were most likely due to the heterogenicity of the stream bed.

Barring effects from streambed heterogenicity, EPC_o results indicated that La Jara Creek's riverbed could oscillate between being a sink or a source of P to water column as a function of Q. It should be noted, however, that it remains to be known if observed differences in EPC_o before and after a single high flow event are significant, as the sample size was too small to conduct meaningful statistics. As such, the riverbed's

sorption status was determined for the upper and lower reaches individually with relation to water column SRP concentrations and Q (cfs). Regression analysis showed that the sediment's EPC_0 was correlated with the water column's Q at the time of sediment sampling ($p=0.09$) (Table 1.1 & Fig. 1.4), with the riverbed commonly acting as a P source during higher Q's and a sink during lower Q's. For summer 2021 and spring 2022, results for both the lower and upper reaches indicate that the riverbed was behaving as a source of P to the water column during the summer of 2021. This is evident by the lower reach having an EPC_0 range of 5.74-6.92 ($\mu g \cdot L^{-1}$), greater than the water column's SRP concentration of range of 2.20-2.50 ($\mu g \cdot L^{-1}$). Additionally, the upper reach had an EPC_0 range of 6.69-9.47 ($\mu g \cdot L^{-1}$) and an SRP concentration of 2.20-2.80 ($\mu g \cdot L^{-1}$). Throughout

Sample ID	EPC_0 ($\mu g \cdot L^{-1}$)	Ambient SRP ($\mu g \cdot L^{-1}$)	Source or Sink?	Q (cfs)
LM 7/16/21	5.74	2.50	Source	1.14
UM 7/16/21	9.47	2.20	Source	1.14
LM 7/27/21	6.92	2.80	Source	1.22
UM 7/27/21	6.69	2.80	Source	1.22
LM 3/13/22	5.97	4.09	Source	0.14
UM 3/13/22	2.29	4.52	Sink	0.14
LM 3/18/22	1.15	4.37	Sink	0.15
UM 3/18/22	3.79	6.58	Sink	0.15
LM 4/1/22	1.51	4.15	Sink	0.33
UM 4/1/22	3.47	3.27	Source	0.33
LT 7/12/22	2.21	1.66	Source	1.12
UT 7/12/22	2.61	2.18	Source	1.12
LT 8/4/22	1.42	2.86	Sink	0.72
UT 8/4/22	2.25	2.86	Sink	0.72

Table 1.1: Comparison of EPC_0 ($\mu g \cdot L^{-1}$) to water column SRP content ($\mu g \cdot L^{-1}$). Sample ID is the Upper (U) or Lower (L) reach sampled, reach Top (T) or Middle (M) areas, and sampling date. Discharge (Q) is presented in cubic feet per second (cfs).

spring 2022, the riverbed's EPC_0 varied across time for both reaches. Although the lower reach started the season as a source, with an EPC_0 of 5.97 and an SRP of 4.10 ($\mu g \cdot L^{-1}$), it shifted to a sink for the rest of the season with an EPC_0 range of 1.15-1.51 ($\mu g \cdot L^{-1}$) and

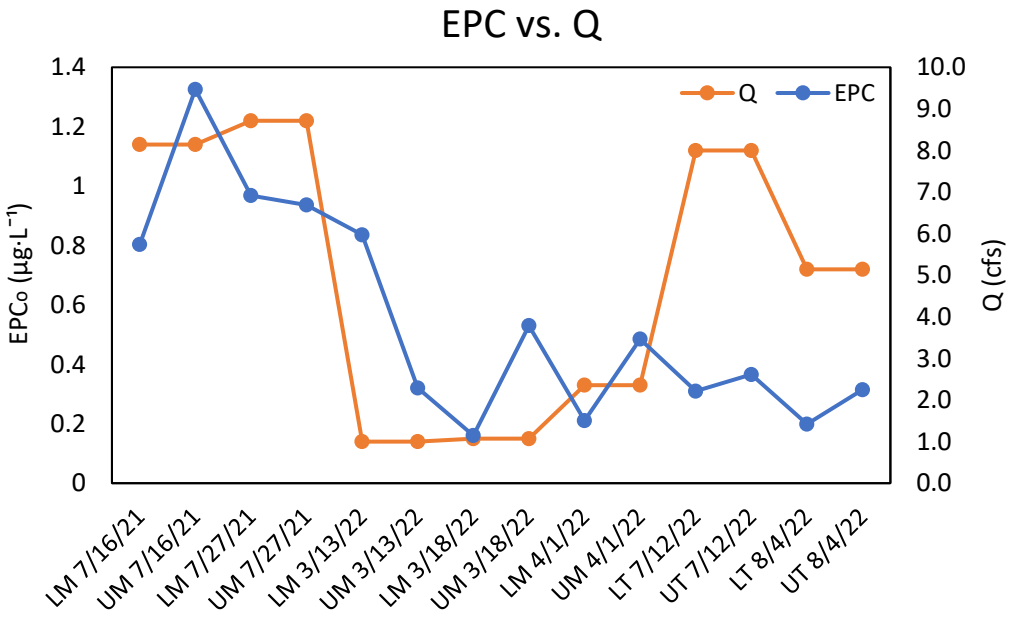

Figure 1.4: Comparison of EPC_0 ($\mu g \cdot L^{-1}$) to water column Q (cfs) at time of sediment sampling. Sample ID is the Upper (U) or Lower (L) reach sampled, reach Top (T) or Middle (M) areas, and sampling date.

an SRP range of 4.20-4.40 ($\mu g \cdot L^{-1}$). The upper reach, however, began the season as a sink with an EPC_0 range of 2.29-3.79 ($\mu g \cdot L^{-1}$) and an SRP concentration of between 4.50-6.60 ($\mu g \cdot L^{-1}$). It then became a source of P to the water column by the end of the season with an EPC_0 of 3.47 and an SRP of 3.30 ($\mu g \cdot L^{-1}$). Summer 2022 results indicate that both reaches shifted from behaving as a source of P to the water column prior to the first armor moving storm on 8/3/22, to being a sink on 8/4/22. Both the lower and upper reaches had an EPC_0 of 2.21 ($\mu g \cdot L^{-1}$) and 2.61 ($\mu g \cdot L^{-1}$), respectively, greater than their

respective SRP concentrations of 1.70 and 2.20 ($\mu g \cdot L^{-1}$). This indicates that both reaches were acting as a source at the beginning of the sampling season. Samples collected after the first armor-moving storm of the season (Storm 2) showed that both reaches shifted to behaving as a sink, with the lower reach having an EPC_o of 1.42 ($\mu g \cdot L^{-1}$), less than its SRP concentration of 2.90 ($\mu g \cdot L^{-1}$), and the upper reach having an EPC_o of 2.25 ($\mu g \cdot L^{-1}$), also less than its SRP of 2.90 ($\mu g \cdot L^{-1}$).

We had enough samples to run statistics between individual seasons and found that on average, the riverbed acted as a source during the summers (Table 1, Figure 4), as differences in streambed EPC_o concentrations between monsoonal years (~1 calendar year) were found to be significant ($p=0.00^{***}$). We used superscripts to denote the degree of certainty of all obtained p-values with $p<0.05^{*}$, $p<0.01^{**}$, and $p<0.001^{***}$. Overall, p-values became increasingly significant as the amount of time between riverbed sampling increased. This is evident in that the average EPC_o for Summer 2021 was significantly lower than that of Summer 2022 with an average difference of 3.90 $\mu g \cdot L^{-1}$ and a $p=0.00^{***}$; Summer 2021 values were less than those of Spring 2022 with difference of 5.08 $\mu g \cdot L^{-1}$ ($p=0.01^{**}$); finally, the least significant difference was found between the Spring 2022 and Summer 2022 sampling periods with an average decrease of 1.19 $\mu g \cdot L^{-1}$ ($p=0.36$).

4. DISCUSSION

Our study set out to understand how armor layer movement influences the mobility of streambed P. Sample collection during both the dam release experiments and key parts of the natural storms' hydrograph allowed us to establish P hysteresis directionality and determine P's primary source. Though sample storms were limited, our data broadly suggest that the frequency and intensity of storms may influence P mobility from stream sediments.

Our data suggest that antecedent conditions of a riverbed and its respective watershed could be the likely drivers of armor layer disturbance and P mobility during high flow events. However, more research is required to test this hypothesis as the sample size of our study is small. La Jara Creek's riverbed only had a five-day recharge period for P accumulation before Storm 3 occurred and resulted in opposing hysteresis patterns when compared to storms 1-2, both of which had recharge periods of over a month. Additionally, while both dam release experiments had similar peak Q's, E5.U reached its peak in TP about 20 seconds faster than E1.U, suggesting that the armor layer experienced a decrease in stability over the course of the experiments, allowing for a more rapid release of TP. These results support both $\mathbf{HY_1}$ and $\mathbf{HY_2}$ as armor layer disturbance and subsequent fine sediment exposure did, in fact, lead to changes in the stream P concentrations as well as P hysteresis pattern directionality. As a stream experiences prolonged periods between armor-moving storms, its riverbed can become increasingly stabilized (Chow et al., 2017; Ockelford et al., 2013; Frazar et al., 2019). This increased armor layer resilience is due to the extended time the armor has to settle

and stabilize on the riverbed during normal or low flow conditions between storms. In addition, the longer the armor layer remains stable, the more fine grained, nutrient-rich sediments may accumulate below and within the armor layer (Noonan et al., 2016; Outram et al., 2016). This stabile time period can allow for significant P accumulation below the armor layer as hyporheic flow, organic matter decomposition, and redox reactions with sediment-P increase P stores over time (Sawyer et al., 2012; Drummond et al., 2017). Once an armor-moving, high-flow event occurs, the armor layer is disrupted, leading to the release of accumulated P into the water column and a depletion of P stores within the sediment (Noonan et al., 2016; Outram et al., 2016). This release can often be the dominant source of P, resulting in clockwise hysteresis patterns (Bowes et al., 2005; Chow et al., 2017) as obtained from Storms 1 and 2, supporting **HY_1** and **HY_2**. Due to the depletion of the riverbed's P stores, any future storms that occur shortly thereafter can result in counterclockwise hysteresis patterns as the dominant source of P shifts to coming from overland flow via runoff and hyporheic flux (Vidon et al., 2011; Chow et al., 2017; Correll et al., 1999). Therefore, despite storm 3 being our most intense storm, the 5-day period could have been too short for restabilization of the armor and accumulation of P to occur.

Our results also suggest that antecedent moisture conditions can drive P's transport through a watershed as well, which can then further influence P hysteresis pattern directionality, supporting **HY_2**. While the 2021 and 2022 sampling seasons were both wetter than average, Storm 3 was the most intense storm to pass over La Jara Creek in over a month and potentially increased the watershed's subsurface hydraulic connectivity. As a watershed experiences an intense storm, previously dry subsurface

flow pathways that contribute to streams can suddenly be in use, ultimately increasing the availability and distribution of accumulated P via leaching (Biron et al. 1999; Davis et al., 2014; Noonan et al., 2016). The longer these flow pathways have remained unused, the more legacy P is allowed to accumulate over time. Then, as new water infiltration occurs, the accumulated P can be flushed out into streams via leaching and hyporheic flux from higher water tables (Bowes et al., 2005; Outram et a., 2015; Soulsby et al., 1995), which was most likely what occurred in the La Jara Creek's watershed before/during Storm 3. A lack of intense storms can also lead to the pooling of nutrients above ground in the form of decaying organic matter, sediment, and other particulates. These pools of P can be mobilized when an intense storm occurs and be transported to the stream via runoff (Davis et al., 2014; Frazar et al., 2019; Chen et al., 2015). Thus, the depletion of riverbed P from previous storms in conjunction with the mobilization of overland P could be why storm 3 resulted in TP, SRP, and PP primarily being sourced from distal locations. This theory is further supported in that the results and environmental conditions of our study site correspond with the discussed phenomena and are similar to the findings of studies conducted by Biron et al. (1999), and Davis et al. (2014). Therefore, our findings suggest that the antecedent conditions of a watershed can greatly impact the directionality of P hysteresis patterns in rivers during high flow events, supporting **HY_2**.

EPC_0 results imply that the riverbed has the capacity to oscillate between acting as a source or sink of P to the water column. Thus, **HY_2** is supported in that the P composition of mobilized fine sediment can indeed influence SRP bioavailability and hysteresis patterns. During high flow events, riverbed sediments can affect P hysteresis patterns through sorption or desorption to/from sediment exchange sites. Additionally,

our sequential extraction results showed no significant difference in P concentrations across time or space. The observed shift in the riverbed's EPC_0 from source to sink after Storm 3, however, potentially suggests that fine sediment disruption can influence P bioavailability and hysteresis patterns during high flow events. But it should again be noted that it remains to be known if this observed shift in EPC_0 between the start and end of a single season are significant as the sample size was too small to conduct meaningful statistics. As such, the riverbed's sorption status was determined in relation to water column SRP as previously described. These results agree with a study conducted by Son et al., (2015), where monitored streams oscillated between source and sink as disturbances led to frequent changes in sediment sorption status. As previously discussed, these changes in sorption status can lead to the accumulation of P in the riverbed if the armor layer remains undisturbed (Noonan et al., 2016; Outram et al., 2016). A perpetual lack of armor-disturbing events can allow P accumulation to persist, increasing the likelihood of its release to the water column, ultimately resulting in the riverbed becoming a source of P (Son et al., 2015; Pant et al., 2002). If the riverbed is behaving as a P source when an armor-moving storm occurs, it can result in biogeochemical reactions that causes sediment grains to release sorbed P, influencing hysteresis pattern directionality (Sherson et al., 2012; Yan et al., 2020; He et al., 2018; Stone et al., 2004). This release of P can deplete the riverbed's P concentration, which can prompt the riverbed to shift back to behaving as a sink (Sherson et al., 2012; Yan et al., 2020), beginning the cycle anew. The observance of this cycle therefore further supports both $\mathbf{HY_1}$ and $\mathbf{HY_2}$, in that armor layer disturbances can lead to fluctuations in PP and SRP concentrations and subsequently affect hysteresis pattern directionality within streams.

The combination of the above results is what led us to posit that two of the primary drivers behind P mobility during storm events could be the antecedent conditions of both the riverbed and its respective watershed. In addition, because P mobility plays a significant role in nutrient spiraling (Finkler et al., 2021; Ensign & Doyle, 2005), the antecedent conditions of these systems could subsequently influence the movement of P through any of the nutrient spiraling stages, as well. For example, the dry antecedent conditions experienced by La Jara Creek's watershed in the 30+ days leading up to Storm 2 likely allowed for an accumulation of P within the riverbed, as infrequent, minor rainstorms allowed for consistent baseline Q's, facilitating armor layer stabilization (Son et al., 2015; Pant et al., 2002). As previously discussed, these factors likely promoted a "sink" sorption status for the riverbed, as the potential for P release into the water column increased with the gradual P accumulation over time (Son et al., 2015; Pant et al., 2002; Sherson et al., 2012; Yan et al., 2020). These antecedent conditions, coupled with the rainfall and runoff of Storm 2, can heavily influence P nutrient spiraling patterns as a result of increased P mobility, which can impact the transport, uptake, transformation, and overall bioavailability of P throughout these systems as the armor layer and other watershed P stores are disturbed (Yan et al., 2019, 2020; Buckingham et al., 2010; He et al., 2018; Correll et al., 1999). The frequency and intensity of armor-disturbing rainstorms is just one of the many antecedent conditions that can significantly impact P mobility and subsequent nutrient spiraling patterns within stream networks (Outram et al., 2016; Bowes et al., 2005). Therefore, understanding the effects of antecedent conditions of watersheds and riverbeds as a whole could allow for better maintenance of sensitive nutrient spiraling patterns as well as management of water quality issues.

It is widely accepted that changes in the Earth's climate have led to a rise in severe weather events (Bruine de Bruin Wandi et al., 2022; IPCC, 2014). In particular, the hydrologic cycle has been affected as rain patterns have shifted from periodic, mild events to irregular, intense storms (File et al., 2020; Zhou et al., 2018). The perpetuation of this shift can affect a watershed's antecedent conditions and nutrient spiraling patterns, producing optimal conditions for P accumulation during the dry periods. As such, the future occurrence of less frequent, high intensity storms could produce higher rates of P transport through watersheds, exacerbate P release from increased armor layer disturbance in streams, and ultimately lead to changes in stream P concentrations.

5. CONCLUSION

The findings of this study highlight the significant role of antecedent conditions of a riverbed and its respective watershed in driving armor layer disturbance and P mobility during high flow events. Climate change-induced shifts in rain patterns can affect these antecedent conditions, leading to depletion of riverbed P from previous storms and mobilization of overland P, which can result in distal locations becoming the primary source of P. This release of P can cause oscillations in the riverbed's status as a source or sink relative to the overlying water column, leading to hysteresis patterns within streams that are influenced by riverbed sediment composition. These findings emphasize the complex interaction between hydrological processes, climate change, and riverbed dynamics in shaping nutrient spiraling in river ecosystems. Further research in this area is crucial for a better understanding of the implication of these processes on water quality management and ecosystem health.

REFERENCES

Anju, S., Green, M. B., Boyer, J. N., & Doner, L. A. (2020). Effects of storm events on phosphorus concentrations in a forested new england stream. *Water, Air and Soil Pollution, 231*(7). doi:https://doi.org/10.1007/s11270-020-04738-0

Atkinson, C. L., van Ee, B.,C., Lu, Y., & Zhong, W. (2019). Wetland floodplain flux: Temporal and spatial availability of organic matter and dissolved nutrients in an unmodified river. *Biogeochemistry, 142*(3), 395-411. doi:https://doi.org/10.1007/s10533-019-00542-z

Biron, P.M., A.G. Roy, F. Courchesne, W.H. Hendershot, B. Cote, and J. Fyles. 1999. The effects of antecedent moisture conditions on the relationship of hydrology to hydrochemistry in a small forested watershed. *Hydrol. Processes, 13*, 1541–1555. doi:10.1002/ (SICI)1099-1085(19990815)13:11<1541::AID-HYP832>3.0.CO;2-J

Bowen, B.M. (1996). Rainfall and climate variation over a sloping New Mexico plateau during the North American monsoon. *Journal of Climate*, *9*(12): 3432–3442.

Bowes, M. J., House, W. A., Hodgkinson, R. A., & Leach, D. V. (2005). Phosphorus-discharge hysteresis during storm events along a river catchment: The river swale, UK. *Water Research, 39*(5), 751-762. Retrieved from https://login.dist.lib.usu.edu/login?url=https://www-proquest-com.dist.lib.usu.edu/scholarly-journals/phosphorus-discharge-hysteresis-during-storm/docview/67486714/se-2?accountid=14761

Brooks, .PD., Vivoni, E.R. (2008). Mountain Ecohydrology: Quantifying the role of vegetation in the water balance of montane catchments. *Ecohydrology*, *1*, 187–192.

Broxton, P.D., Troch, P.A., Lyon, S.W. (2009). On the role of aspect to quantify water transit times in small mountainous catchments. *Water Resour Res, 45*(8):W08427.

Bruine de Bruin Wändi, & Dugan, A. (2022). On the differential correlates of climate change concerns and severe weather concerns: Evidence from the world risk poll. *Climatic Change, 171*(3-4). doi:https://doi.org/10.1007/s10584-022-03353-8

Buckingham, S. E., Neff, J., Titiz-maybach, B., & Reynolds, R. L. (2010). Chemical and textural controls on phosphorus mobility in drylands of southeastern utah. *Biogeochemistry, 100*(1-3), 105-120. doi:https://doi.org/10.1007/s10533-010-9408-7

Chen, D., Hu, M., Guo, Y., & Dahlgren, R. A. (2015). Influence of legacy phosphorus, land use, and climate change on anthropogenic phosphorus inputs and riverine export dynamics. *Biogeochemistry, 123*(1-2), 99-116. doi:https://doi.org/10.1007/s10533-014-0055-2

Chow, M. F., Huang, J., & Shiah, F. (2017). Phosphorus dynamics along river continuum during typhoon storm events. *Water, 9*(7). doi:https://doi.org/10.3390/w9070537

Correll, D. L., Jordan, T. E., & Weller, D. E. (1999). Transport of nitrogen and phosphorus from rhode river watersheds during storm events. *Water Resources Research, 35*(8), 2513-2521. doi:https://doi.org/10.1029/1999WR900058

Davis, C. A., Ward, A. S., Burgin, A. J., Loecke, T. D., Riveros-Iregui, D., Schnoebelen, D. J., . . . St Clair, M.,A. (2014). Antecedent moisture controls on stream nitrate flux in an agricultural watershed. *Journal of Environmental Quality, 43*(4), 1494-1503. Retrieved from https://login.dist.lib.usu.edu/login?url=https://www.proquest.com/scholarly-journals/antecedent-moisture-controls-on-stream-nitrate/docview/1550132942/se-2

Drummond, J. D., Larsen, L. G., R, G., Packman, A. I., & Harvey, J. W. (2017). Fine particle retention within stream storage areas at base flow and in response to a storm event. *Water Resources Research, 53*(7), 5690-5705. doi:https://doi.org/10.1002/2016WR020202

Ensign, S. H., and Doyle, M. W. (2006), Nutrient spiraling in streams and river networks, *J. Geophys. Res.*, *111*, G04009, doi:10.1029/2005JG000114.

File, D. J. M., & Derbile, E. K. (2020). Sunshine, temperature and wind: Community risk assessment of climate change, indigenous knowledge and climate change adaptation planning in ghana. *International Journal of Climate Change Strategies and Management, 12*(1), 22-38. doi:https://doi.org/10.1108/IJCCSM-04-2019-0023

Finkler, N., Gücker, B., Iola Gonçalves Boëchat, Tromboni, F., Steven, A. T., Ludmilson, A. M., . . . Davi Gasparini, F. C. (2021). Comparing spiraling- and transport-based approaches to estimate in-stream nutrient uptake length from pulse additions. *Ecohydrology, 14*(7). doi:https://doi.org/10.1002/eco.2331

Frazar, S., Gold, A. J., Addy, K., Moatar, F., Birgand, F., Schroth, A. W., . . . Pradhanang, S. M. (2019). Contrasting behavior of nitrate and phosphate flux from high flow events on small agricultural and urban watersheds. *Biogeochemistry, 145*(1-2), 141-160. doi:https://doi.org/10.1007/s10533-019-00596-z

Gustafson, J. R., Brooks, P. D., Molotch, N. P., & Veatch, W. C. (2010). Estimating snow sublimation using natural chemical and isotopic tracers across a gradient of solar radiation. *Water Resources Research, 46*(12), Citation W12511. doi:https://doi.org/10.1029/2009WR009060

He, S., & Xu, Y. J. (2018). Phosphorus fluxes from three coastal watersheds under varied agriculture intensities to the northern gulf of mexico. *Water, 10*(6), 816. doi:https://doi.org/10.3390/w10060816

Hongthanat, N. (2010). Phosphorus sorption-desorption of soils and sediments in the Rathbun Lake watershed. Iowa State University Digital Repository, https://doi.org/10.31274/etd-180810-2127

House, W. A. (2003). Geochemical cycling of phosphorus in rivers. *Applied Geochemistry, 18*(5), 739-748. Retrieved from https://login.dist.lib.usu.edu/login?url=https://www-proquest-com.dist.lib.usu.edu/docview/19813174?accountid=14761

IPCC (2014) Climate change 2014: synthesis report. Contribution of Working Groups I, II and III to the Fifth Assessment Report of the Intergovernmental Panel on Climate Change [Core Writing Team, R.K. Pachauri and L.A. Meyer (eds.)]. IPCC, Geneva, Switzerland. https://www.ipcc.ch/report/ar5/syr/. Accessed 10 Apr 2023

Jarvie, H. P., Neal, C., & Withers, P. J. A. (2006). Sewage-effluent phosphorus: A greater risk to river eutrophication than agricultural phosphorus? *Science of the Total Environment, 360*(1-3), 246-253. doi:https://doi.org/10.1016/j.scitotenv.2005.08.038

Johnson, D. W., Walker, R. F., McNulty, M., Rau, B. M., & Miller, W. W. (2012). The long-term effects of wildfire and post-fire vegetation on sierra nevada forest soils. *Forests, 3*(2), 398-416. doi:https://doi.org/10.3390/f3020398

Kelly, P. T., Renwick, W. H., Vanni, M. J., & Knoll, L. (2019). Stream nitrogen and phosphorus loads are differentially affected by storm events and the difference may be exacerbated by conservation tillage. *Environmental Science & Technology, 53*(10), 5613-5621. doi:https://doi.org/10.1021/acs.est.8b05152

Kerr, J. G., Burford, M. A., Olley, J. M., Bunn, S. E., & Udy, J. (2011). Examining the link between terrestrial and aquatic phosphorus speciation in a subtropical catchment: The role of selective erosion and transport of fine sediments during storm events. *Water Research, 45*(11), 3331-3340. doi:https://doi.org/10.1016/j.watres.2011.03.048

Lapworth, D. J., Gooddy, D. C., & Jarvie, H. P. (2011). Understanding phosphorus mobility and bioavailability in the hyporheic zone of a chalk stream. *Water, Air and Soil Pollution, 218*(1-4), 213-226. doi:https://doi.org/10.1007/s11270-010-0636-1

Liu F, Parmenter R, Brooks PD, Conklin MH, Bales RC (2008). Seasonal and interannual variation of streamflow pathways and biogeochemical implications in semi-arid, forested catchments in Valles Caldera, New Mexico. *Ecohydrology, 1*(3):239–252.

Lottig, N. R., & Stanley, E. H. (2007). Benthic sediment influence on dissolved phosphorus concentrations in a headwater stream. *Biogeochemistry, 84*(3), 297-309. doi:https://doi.org/10.1007/s10533-007-9116-0

McIntosh, J. C., Schaumberg, C., Perdrial, J., Harpold, A., Angélica Vázquez-Ortega, Rasmussen, C., Chorover, J. (2017). Geochemical evolution of the critical zone across variable time scales informs concentration-discharge relationships: Jemez river basin critical zone observatory. *Water Resources Research, 53*(5), 4169. doi:https://doi.org/10.1002/2016WR019712

Noonan, B. J. (2016). *Stream channel erosion as a source of sediment and phosphorous in a central iowa stream* (Order No. 10126563). Available from Agricultural & Environmental Science Collection. (1797608854). Retrieved from https://login.dist.lib.usu.edu/login?url=https://www-proquest-com.dist.lib.usu.edu/dissertations-theses/stream-channel-erosion-as-source-sediment/docview/1797608854/se-2?accountid=14761

Ockelford, A., & Haynes, H. (2013). The impact of stress history on bed structure: The journal of the british geomorphological research group. *Earth Surface Processes and Landforms, 38*(7), 717-727. doi:https://doi.org/10.1002/esp.3348

Outram, F. N., Cooper, R. J., Sünnenberg, G., Hiscock, K. M., & Lovett, A. A. (2016). Antecedent conditions, hydrological connectivity and anthropogenic inputs: Factors affecting nitrate and phosphorus transfers to agricultural headwater streams. *Science of the Total Environment, 545-546*, 184-199. doi:https://doi.org/10.1016/j.scitotenv.2015.12.025

Pant, H. K., Nair, V. D., Reddy, K. R., Graetz, D. A., & Villapando, R. R. (2002). Influence of flooding on phosphorus mobility in manure-impacted soil. *Journal of Environmental Quality, 31*(4), 1399-1405. Retrieved from https://login.dist.lib.usu.edu/login?url=https://www-proquest-com.dist.lib.usu.edu/scholarly-journals/influence-flooding-on-phosphorus-mobility-manure/docview/16138831/se-2?accountid=14761

Perdrial, J. N., McIntosh, J., Harpold, A., Brooks, P. D., Zapata-Rios, X., Ray, J., Chorover, J. (2014). Stream water carbon controls in seasonally snow-covered mountain catchments: Impact of inter-annual variability of water fluxes, catchment aspect and seasonal processes. *Biogeochemistry, 118*(1-3), 273-290. doi:https://doi.org/10.1007/s10533-013-9929-y

Pierzynski, G. M., Sims, J. T., & Vance, G. F. (1994). Soils and environmental quality. Gary M. Pierzynski, J. Thomas Sims, George F. Vance. Lewis Publishers.

Rinehart, A.J., Vivoni, E.R., Brooks, P.D. (2008). Effects of vegetation, albedo, and solar radiation sheltering on the distribution of snow in the Valles Caldera, New Mexico. *Ecohydrology, 1*(3), 253–270.

Ross, D. S., Wemple, B. C., Willson, L. J., Balling, C. M., Underwood, K. L., & Hamshaw, S. D. (2019). Impact of an extreme storm event on river corridor bank erosion and phosphorus mobilization in a mountainous watershed in the northeastern united states. *Journal of Geophysical Research.Biogeosciences, 124*(1), 18-32. doi:https://doi.org/10.1029/2018JG004497

Sawyer, A. H., & Cardenas, M. B. (2012). Effect of experimental wood addition on hyporheic exchange and thermal dynamics in a losing meadow stream. *Water Resources Research, 48*(10). doi:https://doi.org/10.1029/2011WR011776

Sherson, L.R. (2012). Nutrient dynamics in a headwater stream: use of continuous water quality sensors to examine seasonal, event, and diurnal processes in the East Fork

Jemez River, NM. M.S. thesis. Department of Earth and Planetary Sciences, University of New Mexico.

Stone, M., & English, M.C. (2004). Geochemical composition, phosphorus speciation and mass transport of fine-grained sediment in two Lake Erie tributaries. *Hydrobiologia, 253*, 17-29.

Son, J., Kim, S., & Carlson, K. H. (2015). Effects of wildfire on river water quality and riverbed sediment phosphorus. *Water, Air and Soil Pollution, 226*(3), 1-13. doi:https://doi.org/10.1007/s11270-014-2269-2

Soulsby, C. 1995. Contrasts in storm event hydrochemistry in an acidic a forested catchment in upland Wales. *J. Hydrol. 170*, 159–179. doi:10.1016/0022-1694(94)02677-4

Vidon, P., & Cuadra, P. E. (2011). Phosphorus dynamics in tile-drain flow during storms in the US midwest. *Agricultural Water Management, 98*(4), 532-540. doi:https://doi.org/10.1016/j.agwat.2010.09.010

Webster, J. (1975). Analysis of potassium and calcium dynamics in stream ecosystems on three Southern Appalachian watersheds of contrasting vegetation, Ph.D. dissertation, Univ. of Ga. at Athens, Athens.

Xue, L., Li, Q., & Chen, H. (2014). Effects of a wildfire on selected physical, chemical and biochemical soil properties in a pinus massoniana forest in south china. *Forests, 5*(12), 2947-2966. doi:https://doi.org/10.3390/f5122947

Yan, W., Liu, L., Wu, T., Song, L., Wang, H., Lu, Z. Zhu, Y. (2019). Effects of short-term aerobic conditions on phosphorus mobility in sediments. *Journal of Freshwater Ecology, 34*(1), 649-661. doi:https://doi.org/10.1080/02705060.2019.1659190

Yan, W., Chen, M., Fan, K., Liu, L., Wang, H., Wu, T., Zhang, Y. (2020). Mechanism of phosphorus mobility in sediments with larval (propsilocerus akamusi) bioturbation. *Environmental Science and Pollution Research International, 27*(7), 7538-7548. doi:https://doi.org/10.1007/s11356-019-07404-z

Zapata-Rios, X., Troch, P.A., McIntosh, J., Broxton, P., Harpold, A.A., Brooks, P.D. (2012). When winter changes: differences in the hydrological response from first-order catchments of similar age in New Mexico. American Geophysical Union Fall Meeting, San Francisco.

Zhou, A., Tang, H., & Wang, D. (2005). Phosphorus adsorption on natural sediments: Modeling and effects of pH and sediment composition. *Water Research*, 39(7), 1245–1254. doi:https://doi.org/10.1016/j.watres.2005.01.026

CHAPTER 3: INVESTIGATING THE LONG-TERM EFFECTS OF WILDFIRE ON STREAM PHOSPHORUS CONCENTRATIONS

1. INTRODUCTION

Wildfires can be one of nature's most severe natural disasters yet can play a crucial role in ecosystem health. Watersheds affected by wildfires often undergo changes in ecological properties that result in changes to nutrient flux and transport (Xue et al., 2014; Johnson et al., 2012). A key nutrient influenced by fire is phosphorus (P), a limiting nutrient for most flora as it promotes the growth of plants and aquatic algae in waterways (Chow et al., 2017; Yan et al., 2019; House, 2003; Zhou et al., 2005; Lapworth et al., 2011). As a wildfire burns plants and other organic matter, P can be mobilized as ash or other particulates and made readily available for uptake in topsoil post-fire (Miller et al., 2013; Son et al., 2015; Rust, 2017). However, if this newly available P is not immediately taken up by vegetation, it often makes its way into nearby waterways via runoff from storms, effectively increasing stream P loads for years after (Miller et al., 2012; Lagerstroem et al., 2009; Son et al., 2015), often in a very dramatic fashion with increases of up to 200% (Rust, 2017; Spracklen et al., 2009). If these increased P loads persist for extended periods of time, it can negatively shift community composition (He et al., 2019; Noonan et al., 2016) by leading to a dominance of undesirable species, which can influence the trophic transfer of nutrients or, in extreme cases, promote the proliferation of toxic cyanobacterial species that can poison animals and degrade habitats (Larson et al., 2020; Frazar et al., 2019).

Wildfires can also affect vegetation cover and soil properties as forest canopy and organic surface litter are burned, increasing the soil's water repellency and ultimately decreasing soil water holding capacity and limiting soil-water interaction times (Ice et al., 2004; Rust, 2017; Xue et al., 2014). These effects are often determined by the fire's duration and intensity (Ice et al., 2004), which, in turn, are often repercussions of droughts due to climate change (Xue et al., 2014). Climate change has also continued to increase the occurrence of wildfires as land area burned is projected to increase by 50-100% within the next fifty years (Rust, 2017; McKenzie et al., 2004). During the 2017 wildfire season alone, the Western United States experienced a 44% increase in land burned by wildfire when compared to average land area burned just ten years previous (NICC, 2017; Rust, 2017). These wildfire effects significantly increase the likelihood of P mobilization in watersheds as P-rich ash and other particulates are transported to streams by storm runoff and leaching (Son et al., 2015; Qian et al., 2009).

While many studies have looked at immediate changes in a watershed's P export 1-5 years post burn and found significant increases of P in streams (Miller et al., 2013; Noske et al., 2010; Blake et al., 2010), very few have looked at what, if any, changes persist long-term, or 5+ years post wildfire. This issue is highlighted in a meta-analysis conducted by Hampton et al., (2022), which found that of 121 watersheds studied across 34 publications, only 47% of sites were sampled for more than one year, and a mere 9% of sites were sampled for more than 5 years. Of that 9%, most sites focused on analysis of nutrients other than P. As such, the lack of long-term, post-fire sampling regimes has made it difficult to ascertain recovery times of stream network systems 5+ post-burn. A few studies, however, have analyzed long-term changes of P availability in topsoil (Rust,

2017; Xue et al., 2014; Johnson et al., 2012). For example, a study conducted by Johnson et al., (2012) found significant decreases in soil extractable P in forests burned 70 years prior when compared to non-burned soils. An additional study by Xue et al., (2014) found that although available soil P concentrations significantly increased immediately after a fire, they progressively decreased below baseline levels by 4 years post-burn through the end of the study, 7 years post-burn. Xue et al., (2014) then posited that these long-term decreases in soil extractable P could be a result of decreased nutrient availability due to continuous removal from soils via leaching and runoff (Miesel et al., 2012; Wuthrich et al., 2002). This trend could very well lead to significant decreases in stream P availability long-term as overland P sources become increasingly depleted over time. Therefore, the purpose of this study is to determine the validity of **HY_1-** significant differences in stream SRP concentrations persist and are correlated with a watershed's burn severity 9+ years post burn.

2. METHODS

2.1 Study Area

To evaluate the long-term effects of burn severity of P accumulation in streams, we sampled watersheds within a 9-year-old burn scar. Our study area was eight different watersheds within the Valles Caldera National Preserve in Los Alamos, New Mexico (Fig. 1). This Caldera is ~15 km northeast of Jemez Springs and 30 km west of Los Alamos in the northern volcanic Jemez Mountains of northern New Mexico (Liu et al., 2008). The Jemez Mountains are in the transition zone between the snow-dominated Rocky Mountains and the monsoon-dominated southwestern United States, resulting in a bimodal pattern of annual precipitation (Brooks et al., 2008; Perdrial et al., 2013). Elevations range from 2300 m at Redondo Meadow to 3432 m at Redondo Peak. Since the early 1980s, the annual temperature has averaged 9 °C and precipitation averaged 476 mm, as measured in a neighboring site at an elevation of about 2200 m in Los Alamos (Liu et al., 2008; Bowen et al., 1996; Perdrial et al., 2013). Mean precipitation from October to April accounts for 40% of the annual total and falls primarily as snow (Gustafson et al., 2010; Rinehart et al., 2008). Mean precipitation during the monsoon season in July and August represents approximately 50% of the annual precipitation (Liu et al., 2008; Bowen et al., 1996; Sherson et al., 2015). Summer monsoon precipitation events in July through September occasionally lead to sporadic increases in stream discharge, but these are minimal compared to the snowmelt pulse, as much of the summer precipitation returns to the atmosphere via evapotranspiration (Broxton et al., 2009; Liu et al., 2008; Zapata-Rios et al., 2015; McIntosh et al., 2017).

The Thompson Ridge wildfire ignited in the summer of 2013 due to a downed electrical line and burned through the Valles Caldera from May 13, 2013 to July 1, 2013 (Incident Information System, 2013). According to a burn analysis conducted by Galanter et al., (2018), the fire burned 24,000 acres, of which 3% experienced high burn severity, 40% moderate severity, and 57% low severity. Burn severity classifications, as determined by the Thompson Ridge Burn Severity map (Burned Area Emergency Response, 2013; Galanter et al., 2018), included unburned, low, moderate, and high.

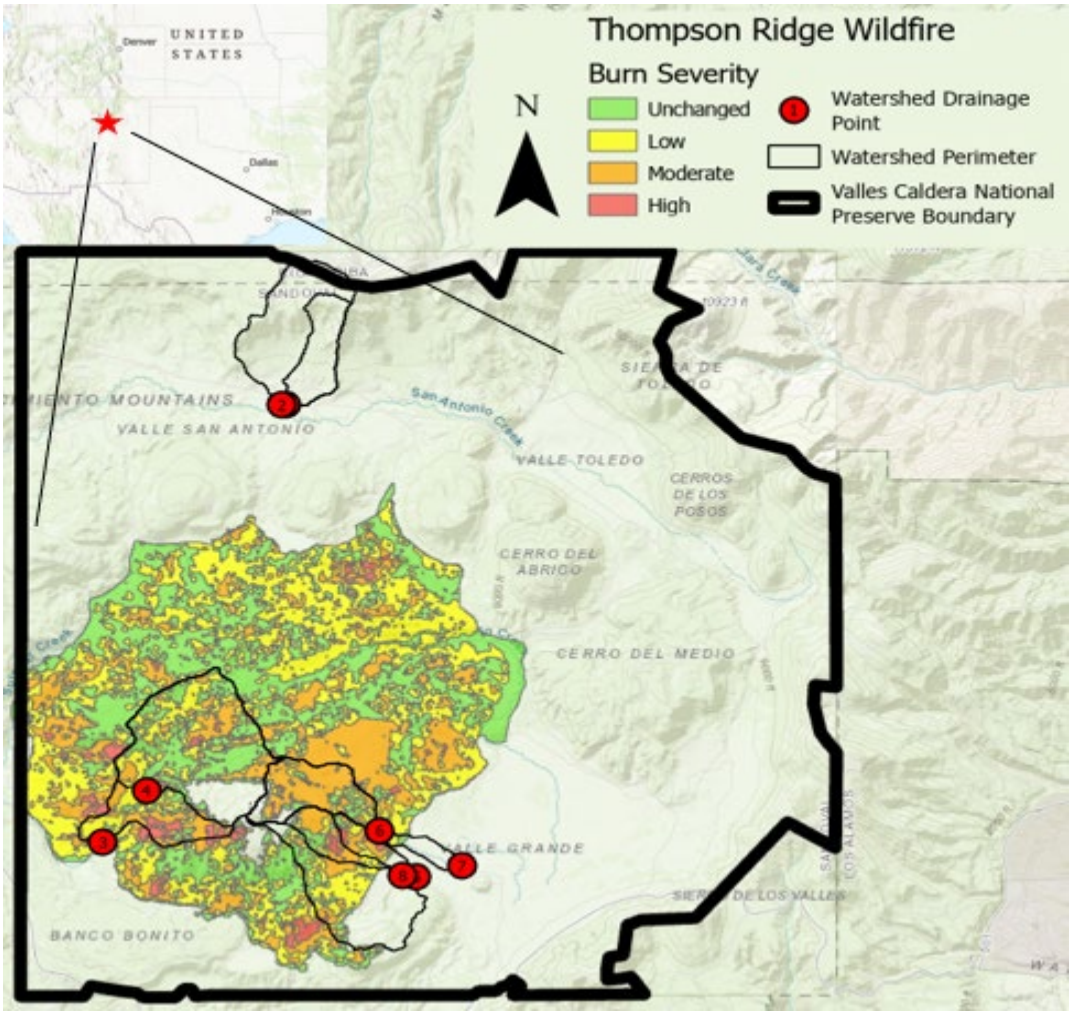

Figure 2.1: Sampling points of the tested watersheds within the Thompson Ridge burn scar in the Valles Caldera National Preserve, New Mexico, USA.

Patches of unburned forest exist within the fire perimeter, and these were included in the analysis. Each of the eight watersheds tested varied in vegetation type, soil permeability, slope, soil water capacity, average drainage area, and elevation.

Each watershed studied was carefully chosen using a combination of analysis via ArcGIS Pro and the USGS Stream Stats application, ensuring that each watershed was similar in area and burn severity distribution. Prospective watersheds were delineated in Stream Stats and transferred as shapefiles to ArcGIS Pro. The Intersect tool was then used to intersect each watershed with the Thompson Ridge fire's burn severity map obtained from the USGS. Burn severities were categorized as Unburned, Low, Moderate, and High based on ArcGIS Pro's Normalized Burn Ratio (NBR), which mathematically compares near and shortwave infrared bands within an image to determine the burn intensity experienced by an area of land during a fire. Next, the ArcGIS Calculate Geometry function was utilized to calculate the percent each watershed was affected by Unburned, Low, Medium, and High burn intensities (Table 2.1). For the experimental control test group, three unburned watersheds that had not been affected by the Thompson Ridge fire were chosen. An additional set of three watersheds with similar distributions of each burn category were chosen to make up a predominately unburned-low burn intensity test group, ranging from 42-52% Unburned, 25-31% Low, 18-23%, and 0-5% High burn intensities (Table 2.1). Another set of three watersheds were chosen in a similar manner to make up a predominately low-moderate burn intensity test group, ranging from 23-35% Unburned, 16-22% Low, 45-58% Moderate, and 0-10% High burn intensities (Table 2.1). As the Thompson Ridge fire had very little high burn area, we were unable to test watersheds that primarily consisted of high burn intensity. In addition

Unburned	Range	Watershed 1	Burn Area (km²)	WATS area burned (%)	WATS area (km²)
Unburned	100%	Unburned	2.70	100.00	
Low	0%	Low			
Moderate	0%	Moderate			
High	0%	High			
		Total	2.70		2.70
Stream Order	WATS #	Watershed 2	Burn Area (km²)	WATS area burned (%)	WATS area (km²)
1	1	Unburned	7.62	100.00	
1	2	Low			
		Moderate			
		High			
		Total	7.62		7.62
Unburned-Low	Range	Watershed 3	Burn Area (km²)	WATS area burned (%)	WATS area (km²)
Unburned	42-52%	Unburned	5.87	42.55	
Low	25-31%	Low	4.22	30.56	
Moderate	18-23%	Moderate	3.13	22.66	
High	0-5%	High	0.58	4.23	
		Total	13.79	100.00	13.79
Stream Order	WATS #	Watershed 4	Burn Area (km²)	WATS area burned (%)	WATS area (km²)
2	3	Unburned	5.38	51.69	
2	4	Low	2.98	28.64	
2	5	Moderate	1.91	18.37	
		High	0.13	1.30	
		Total	8.87	100.00	10.41
		Watershed 5	Burn Area (km²)	WATS area burned (%)	WATS area (km²)
		Unburned	4.47	51.37	
		Low	2.19	25.19	
		Moderate	1.72	19.80	
		High	0.32	3.65	
		Total	5.29	100.00	8.70
Low-Moderate	Range	Watershed 6	Burn Area (km²)	WATS area burned (%)	WATS area (km²)
Unburned	23-35%	Unburned	0.86	23.00	
Low	16-22%	Low	0.68	18.25	
Moderate	45-58%	Moderate	2.14	57.24	
High	0-10%	High	0.06	1.51	
		Total	3.37	100.00	3.73
Stream Order	WATS #	Watershed 7	Burn Area (km²)	WATS area burned (%)	WATS area (km²)
2	6	Unburned	1.61	34.62	
2	7	Low	0.79	16.91	
2	8	Moderate	2.19	47.11	
		High	0.06	1.37	
		Total	4.65	100.00	4.65
		Watershed 8	Burn Area (km²)	WATS area burned (%)	WATS area (km²)
		Unburned	0.36	23.33	
		Low	0.33	21.28	
		Moderate	0.70	45.75	
		High	0.15	9.63	
		Total	1.53	100.00	1.53

Table 2.1: Break down of each sampled watershed's (WATS) stream order and burn severity distribution based on total WATS area (km^2).

to similar burn intensity percentages within test groups, all watersheds chosen for analysis across all test groups had stream orders of 1 or 2, as well as similar watershed drainage areas with an overall range of 1.53-13.79 km^2 (Table 2.1). This was done to ensure that watersheds within each test group were as similar as possible to minimize the effects of heterogeneity.

Stream Stats and ArcGIS Pro were also used to obtain data for parameters that also had the potential to influence P in our chosen watersheds. These parameters include burn severity, stream order, watershed slope, elevation, drainage area, soil permeability, water capacity of the top 1.5 m of soil, vegetation cover type, and annual precipitation. The data for most of the above variables were automatically generated via the Stream Stats program upon delineation of the chosen watershed. Stream order status, however, was obtained by analyzing a digital elevation model (DEM) of the Valles Caldera in ArcGIS Pro using the Fill, Flow Direction, and Flow Accumulation tools. The resulting rasters were input to the Stream to Feature tool to determine the order of each stream we studied.

2.2 Data Collection

We explored **HY_1** by submerging diffusive gradient thin films (DGTs) at the drainage points for nine different watersheds. Each watershed had primarily either unburned, low or moderate burn severities. The DGT binding layers were then analyzed for concentration of SRP trapped to the binding layer and an ANOVA was used to determine if the difference in SRP concentrations between burn severities was significant. Linear regressions were also used to determine if other factors such as annual precipitation, soil water holding capacity and permeability, vegetation type, and drainage

area were influential in the flux of riverine P, measured as the mass of P (ng) that was trapped by the DGT's binding layer as water passed through the device.

2.3 Sample Collection

DGT's were deployed at the drainage point for each watershed. These devices utilized a ferrihydrite binding layer to sorb dissolved P to its surface as the water passed through the device. Using fishing line, three devices were tied into the barrel of a 3 in wide, 1 ft long pvc pipe and submerged underwater for 1-2 days. The temperature of the water was obtained upon device deployment and removal. Once removed from the stream, the DGT's were thoroughly rinsed with DI water and stored in a plastic bag in a refrigerator.

2.4 Laboratory Analysis

For analysis, the DGTs were disassembled. The binding layer was removed, placed in a centrifuge tube with DI water, and left to soak for one hour. The binding layer then underwent a digestion using 0.25M H_2SO_4 to extract the P from its surface. A modified version of the molybdate blue method was used to analyze each sample to determine the amount of SRP on the binding layer. Once each sample's SRP concentration was determined, Equation 1 was used to obtain the final average mass of P on the 3 DGT binding layers per site.

(Eq. 1) $$M = \frac{C_e(V^{bl}+V_e)}{f_e}$$

C_e = measured concentration of analyte in eluent prior to dilution (ng/mL)

V^{bl} = 0.2, volume of binding layer (mL)

V_e = volume of eluent (mL)

f_e = 1, elution factor

M = mass of analyte on binding layer (ng)

Once the mass of P collected by each DGT was calculated at that site, the values were averaged together to find M- the average mass of P (ng) on the binding later for each burn site. The M for each site was then used in an ANOVA to establish potential statistical significance. Using an $\alpha = 0.017$, a Bonferroni correction was then used to isolate which groups were significantly different from each other while reducing the probability of a type I error.

3. RESULTS

ANOVA results show that the watersheds within a predominately Low-Moderate burn severity had significantly lower P concentrations (p=0.007), with an average decrease of 318.84 ng (62%) when compared to control watersheds (Table 1). Predominately Unchanged-Low severity burn sites had an average decrease of 51.79 ng (10%) when compared to Unburned watersheds (p=0.66) and an increase of 267.05 ng (52%) when compared to watersheds located within the Low-Moderate burn severity scar (p=0.04) (Table 1). Overall, however, the study had very low statistical power due to its small sample size (n=8). The Low-Moderate burn group was only statistically different from the unburned group. It should also be noted that the unburned category ended up with only two usable control sites, as one site had no flowing water.

Watershed	**M:** x̄ mass of P on binding layer (ng)
1	528.98
2	493.55
3	470.43
4	597.00
5	311.02
6	201.72
7	248.69
8	126.88

Table 2.2: Average mass (ng) of P accumulated on the DGT binding layer. Colored boxes represent the watershed's burn severity. Green=Unburned/Control, Yellow= Unburned-Low, and Orange= Low-Moderate.

A series of linear regression models were conducted on various watershed parameters to determine their possible influence on P flux. These parameters include burn severity, watershed slope, elevation, drainage area, soil permeability, water capacity of the top 1.5 m of soil, vegetation cover type, and annual precipitation. A table with summarized results for all aforementioned parameters can be found in Appendix B (Table B.2). Here, the summarized results for all parameters found to be significant are presented. P mass (ng) was plotted against the weighted averages for the watershed burn

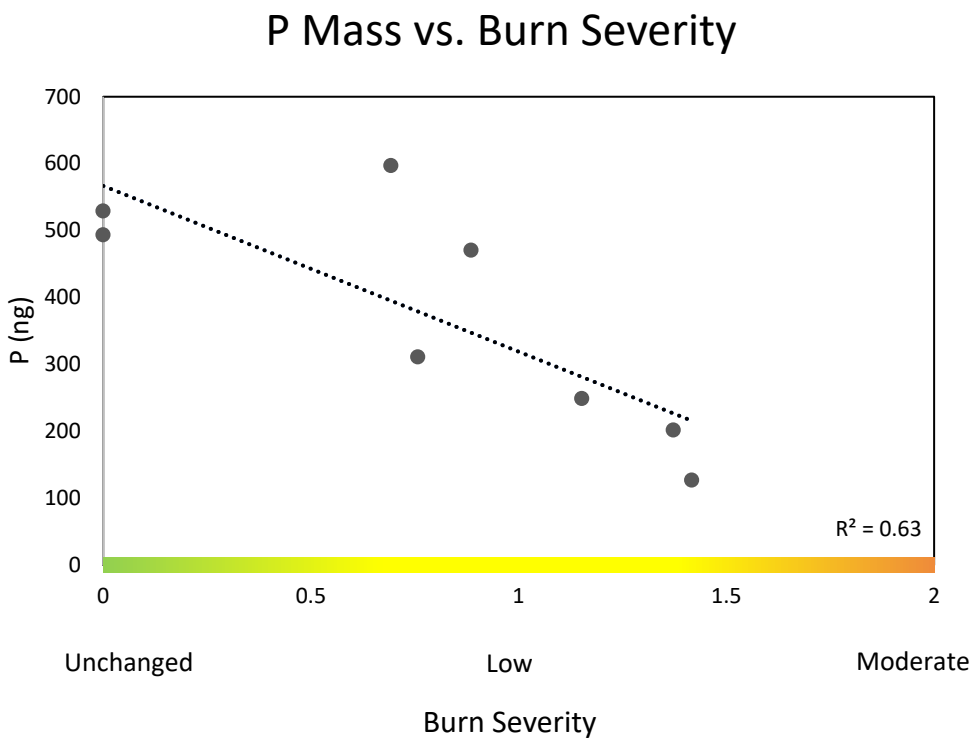

Figure 2.2: Correlation between a watershed's burn severity and average P (ng) accumulated by DGTs.

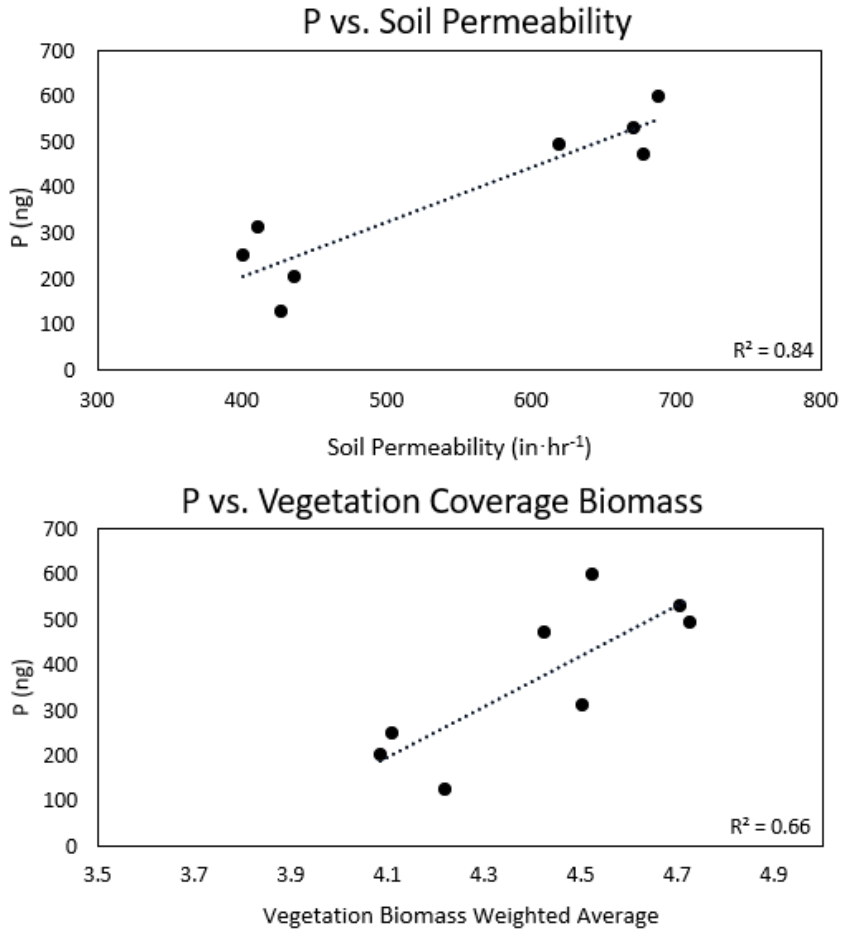

Figure 2.3: Correlation between average P (ng) accumulation and a watershed's elevation and soil permeability (in·hr^{-1}).

severities. The burn severities (Figure 2) were scored as follows; Unburned=0, Low=1, Moderate=2, and High=3. Results showed significance with a correlation coefficient (r) of -0.79 and a p=0.02. Soil Permeability was positively correlated with P accumulation, as well, with an r=0.92 and a p=0.00. The type of vegetation within a watershed was also correlated with P accumulation with an r=0.80 and a p=0.02. Further analysis showed that only two types of vegetation significantly influence P accumulation within a watershed (Fig. B.1, Appendix B). The most influential vegetation was Grassland/Herbaceous, with an r= -0.93 and a p=0.00, followed by Evergreen Forest

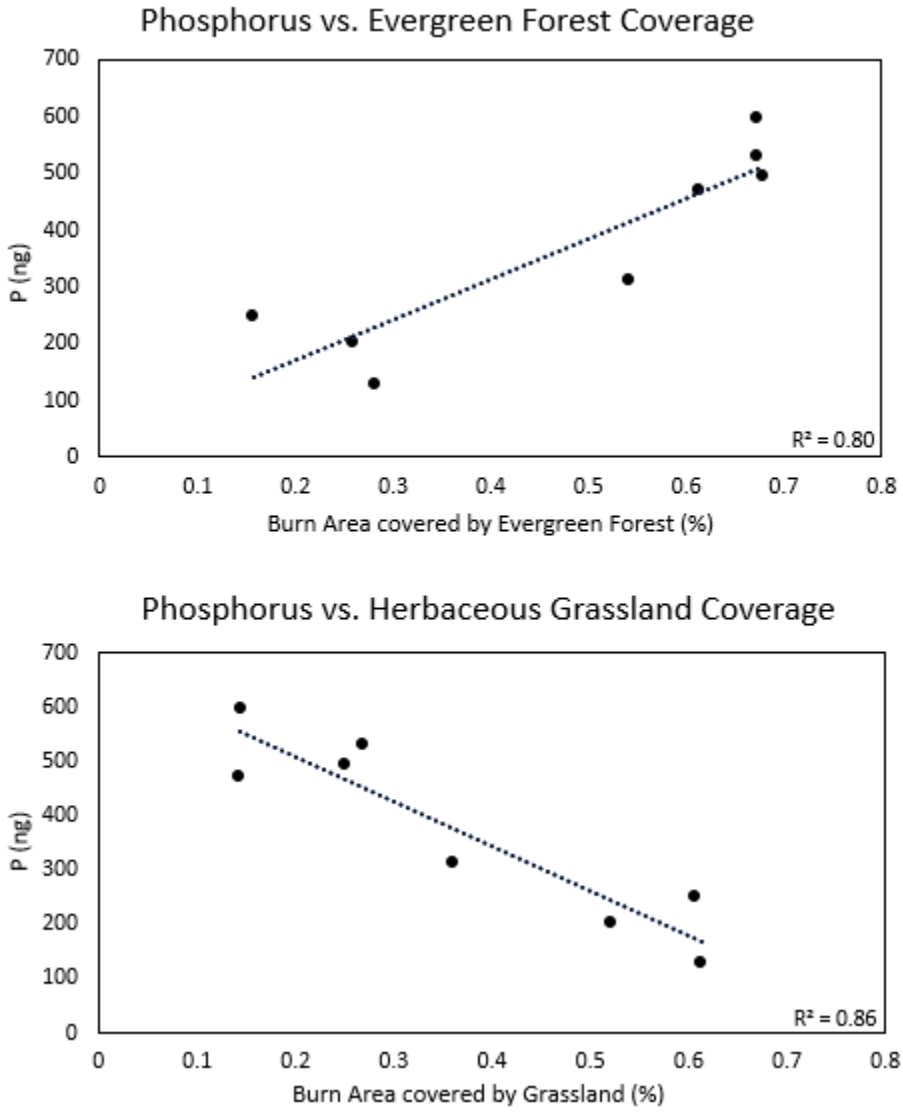

Figure 2.4: Correlation between average P (ng) accumulation and burn area (%) covered significant vegetation types: Evergreen Forest and Herbaceous Grassland.

with an r= 0.89 and a p=0.00. The watershed's elevation was also correlated with P accumulation with an r= -0.64 and p= 0.06. All other parameters were found to be insignificant (Tables B.2 & B.3, Appendix B).

ANOVAs were also used to determine if any significant differences in vegetation coverage persisted 6 years after the fire. The proportion of each experimental watershed

covered by each vegetation type was compared with those found pre-fire (2012) (Table B.3, Appendix B). As expected, there was no significant difference in vegetation coverage within the unburned watersheds between 2012 and 2019. Watersheds that experienced low burn intensities had a significant decrease of 22.70% in evergreen forest coverage ($p<0.01$). Moderately burned watersheds also had a significant decrease of 45.35% in evergreen forest coverage ($p<0.001$), but also had significant increases in herbaceous grassland (+36.43%, $p<0.001$) and shrub/scrub coverage (12.53%, $p<0.05$).

4. DISCUSSION

We deployed DGT's in various streams throughout Valles Caldera National Preserve to determine if changes in P abundance have persisted 9 years post wildfire. P accumulation on these devices showed a significant difference in SRP (ng) between control areas and the Low-Moderate burn severity. A series of linear regressions also indicated a correlation between riverine P flux and burn severity, soil permeability, and the type of vegetation cover. The latter two are both directly influenced by burn severity.

Despite the normal, short-term spikes in stream P concentrations after a fire, our results suggest that P abundance can ultimately decrease long-term, as measured P levels were significantly lower than control concentrations 9 years post burn ($p=0.007<\alpha=0.017$). Our results highlight the long-term effects of burn severity on nutrient concentrations and the oligotrophication of rivers post burn (Table 2.2). To date, no other study has investigated the long-term impacts of wildfire on alpine, riverine systems. As such, our study is the first to observe significant decreases in stream P concentrations over a 9-year period after wildfire occurrence. This observation is supported by previous studies, which found that while wildfires can result in a short-term spike of P abundance at a soil's surface, those levels can decrease back to control concentrations in a few years (Rust, 2017; Xue et al., 2014). These trends led us to posit that changes in stream P levels during the secondary successional process could decrease beyond baseline levels (Fig. 2.5). A significant decrease in P over longer time scales suggests that eutrophication from fires could be a short-term effect while oligotrophication may be a longer-term consequence. Further, this finding raises the question of whether or not watershed slope

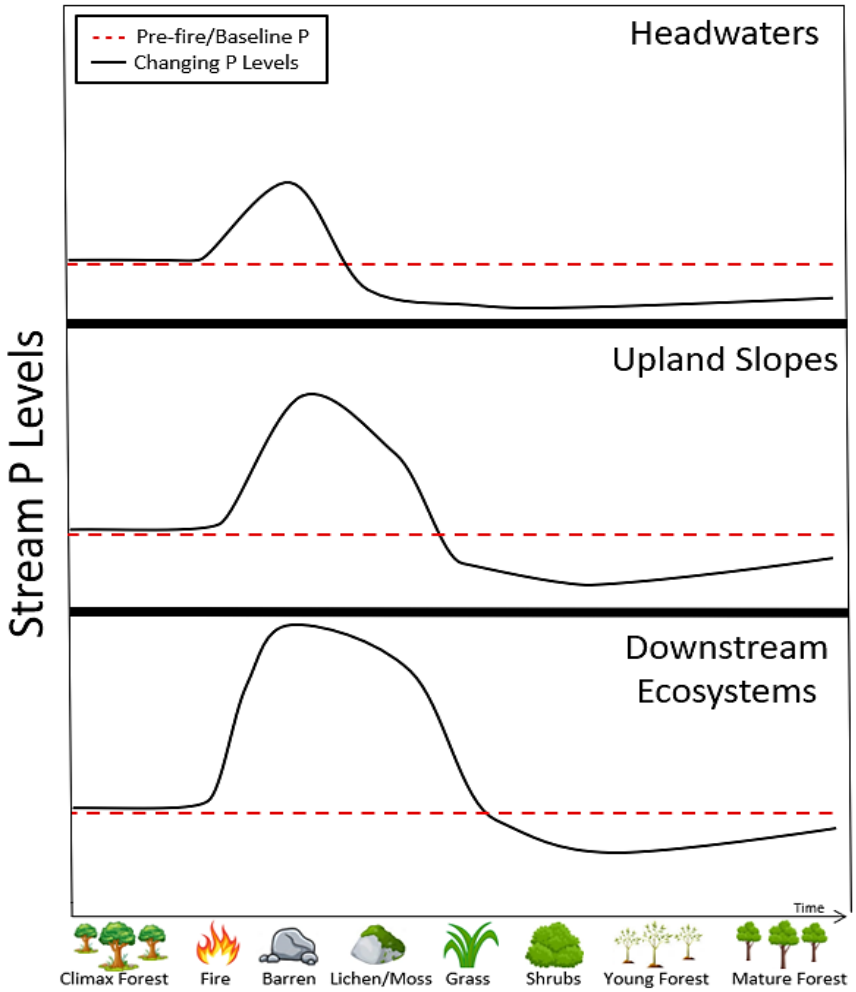

Figure 2.5: Depiction of potential trends in stream phosphorus levels throughout the secondary successional process in three different regions of a watershed: headwaters, upland slopes, and downstream ecosystems (i.e. lakes, reservoirs, and estuaries). Trends are posited based on results from our data and those of other studies. The red dashed line indicates pre-disturbance stream P levels. The solid black line indicates the posited changes in stream P levels over time. After a high intensity wildfire, rates of P loading can get more rapid with travel downstream, as larger, denuded drainage areas affected by destabilized hillslopes are eroded, generating higher Q's and excess sediment/ash bound P (Blake et al., 2010, Prepas et al., 2003). The subsequent fall in P concentrations can become less intense moving downstream as headwater and upland slope locations have smaller drainage areas and steeper slopes when compared to downstream ecosystems (Son et al., 2015; Rust, 2015; Miller et al., 2013). These factors, in conjunction with P uptake by new plant growth, could decrease the probability of P replenishment while simultaneously increasing the transport potential of P already within streams (Son et al., 2015; Blake et al., 2010), ultimately decreasing P levels to below baseline concentrations as found in our study. Finally, we posit that as ecosystem dynamics stabilize throughout the later stages of secondary succession, P levels could potentially remain below baseline levels and exhibit a very slow rise back towards baseline levels, with faster loading rates with movement downstream due to the same factors previously discussed (Johnson et al., 2012; Rust, 2015).

affects the timing of the transition between post-fire P increases to long-term decreases, as loss of fire affected soil can occur more quickly in steeper watersheds (Son et al., 2015; Qian et al., 2009). It is also unknown how these trends influence stream network habitat conditions and nutrient spiraling patterns, or how established recovery patterns will change with increased wildfire frequency induced by climate change.

Our data show a significant relationship between vegetation type and P accumulation ($p=0.02$), which suggests the depletion in P flux could be a result of vegetation recovery during secondary succession, as higher burn intensities lead to more plant loss (Rust, 2017; Johnson et al., 2012). Because P is a limiting nutrient for plant growth, any available P would be taken up during plant propagation throughout the secondary succession process (Lagerstroem et al., 2009; Chow et al., 2017;). This conclusion is further supported by the trend in Figure 2.2, which suggests that a higher burn severity of a watershed can lead to smaller rates of P flux in streams long term. This decrease could be a long-term repercussion of factors related to a fire's burn severity such as the mineralization of P in low intensity fires (Son et al., 2015; Larson et al., 2020), decreased soil permeability (Rust, 2017; Ice et al., 2004), as well as increased P transport via erosion, runoff, and slope degradation (Blake et al., 2010; Son et al., 2015; Frazar et al., 2015), in conjunction with the slow rate of P replenishment from parent material (Ma et al., 2022; Lagerstroem et al., 2009). In addition, because every watershed is unique, each one has different nutrient needs and dynamics. For example, the P needs of vegetation in an alpine watershed could be drastically different from those of a grassland watershed. The combination of these factors suggests that while a fire's burn severity is important, it is not the only parameter that potentially affects P flux within streams long

term. However, it is uncertain whether this finding pertains solely to our tested watersheds or are a trend for watersheds across biomes.

Our results also suggest that the burn severity experienced by a soil can influence the soils permeability, which, in turn, can influence the abundance of P in streams. Of all the linear regressions conducted, the parameter most correlated with P abundance in streams was soil permeability ($r=0.92$, $p=0.001^{***}$), with its trend (Figure 2.3) suggesting that with more intense fires, both P and soil permeability decrease. These results are supported by previous studies which found that intense burns can distort a soils structure and increase its hydrophobicity (Rust, 2017; Debano et al., 2000; Son et al., 2015). This phenomenon occurs as fire spurs pyrolysis in a soil, forming a water repellent layer under the soils surface, effectively reducing a soil's infiltration depth and hydraulic conductivity (Rust, 2017; Debano et al., 2000., Debano et al., 1981). The soil can then become increasingly hydrophobic when subjected to rainstorms as a raindrop's impact and splash can seal a mineral soil's pores at the surface (Ice et al., 2004; Verma et al., 2012), further depleting soil P reserves as it is lost to streams via runoff and leaching short-term (Blake et al., 2010; Ice et al., 2004), thus prompting significant, long-term decreases in stream P concentrations 9 years post-burn.

5. CONCLUSION

The findings of this study highlight the long-term effects of burn severity on P concentrations in rivers post burn. When compared to controls, P concentrations were significantly lower at least 9 years post-burn despite initial spikes in P typically found shortly after a burn event. This persistent difference could be a result of the fire's burn severity and the soil's resulting permeability, as well as changes in landscape vegetation cover. As such, significant differences in stream SRP concentrations post wildfire can persist long term and are correlated with a watershed's burn severity. Future research should focus on sampling more watersheds in both similar and different ecosystems, as well as using a wider variety of burn severities, as this would help provide a more detailed analysis of our observed trends.

CHAPTER 4: GENERAL CONCLUSION

As climate change continues to exacerbate severe and hazardous weather, P becomes increasingly more likely to be mobilized in streams. The combination of wildfires, droughts, and more intense rainstorms, in particular, can influence loading rates of P to streams and lead to short term spikes in overall stream P concentrations. Because P is a key limiting nutrient in watershed systems, these spikes in overall P concentrations can negatively impact production, species composition, and habitat conditions of the ecosystem. As antecedent moisture conditions continue to be affected by drought and higher intensity rainstorms, the overall source of P can shift from proximal to distal sources. Additionally, even though these spikes in P can persist after a wildfire for a short time, our analyses show that they can significantly decrease long-term. This knowledge is important as a better understanding of these trends could foster improvements of strategies for water quality monitoring, restoration efforts, and the protection of natural resources by managing agencies.

REFERENCES

Blake, W. H., Theocharopoulos, S. P., Skoulikidis, N., Clark, P., Tountas, P., Hartley, R., & Amaxidis, Y. (2010). Wildfire impacts on hillslope sediment and phosphorus yields. *Journal of Soils and Sediments*, *10*(4), 671-682. doi:https://doi.org/10.1007/s11368-010-0201-y

Bowen, B.M. (1996). Rainfall and climate variation over a sloping New Mexico plateau during the North American monsoon. *Journal of Climate, 9*(12), 3432–3442.

Brooks, P.D., Vivoni, E.R. (2008). Mountain Ecohydrology: Quantifying the role of vegetation in the water balance of montane catchments. *Ecohydrology, 1*, 187–192.

Broxton, P.D., Troch, P.A., Lyon, S.W. (2009). On the role of aspect to quantify water transit times in small mountainous catchments. *Water Resour Res, 45*(8):W08427.

Chow, M. F., Huang, J., & Shiah, F. (2017). Phosphorus dynamics along river continuum during typhoon storm events. *Water, 9*(7). doi:https://doi.org/10.3390/w9070537

DeBano, L. F., & Pacific Southwest Forest and Range Experiment Station, B. C. (1981). Water repellent soils: a state-of-the-art. Berkeley, Calif. : U.S. Dept. of Agriculture, Forest Service, Pacific Southwest Forest and Range Experiment Station.

DeBano, L. F. (2000). The role of fire and soil heating on water repellency in wildland environments: a review. *Journal of Hydrology*, *231*, 195–206.

Frazar, S., Gold, A. J., Addy, K., Moatar, F., Birgand, F., Schroth, A. W., . . . Pradhanang, S. M. (2019). Contrasting behavior of nitrate and phosphate flux from high flow events on small agricultural and urban watersheds. *Biogeochemistry, 145*(1-2), 141-160. doi:https://doi.org/10.1007/s10533-019-00596-z

Galanter, A., Cadol, D., & Lohse, K. (2018). Geomorphic influences on the distribution and accumulation of pyrogenic carbon (PyC) following a low severity wildfire in northern new mexico: The journal of the british geomorphological research group. *Earth Surface Processes and Landforms, 43*(10), 2207-2218. doi:https://doi.org/10.1002/esp.4386

Gustafson, J.R., Brooks, P.D., Molotch, N.P., Veatch, W.C. (2010). Estimating snow sublimation using natural chemical and isotopic tracers across a gradient of solar radiation. *Water Resour Res, 46*(12):W12511. doi:https://doi.org/10.1029/2009WR009060

Hampton, T. B., Lin, S., & Basu, N. B. (2022). Forest fire effects on stream water quality at continental scales: A meta-analysis. *Environmental Research Letters, 17*(6), 064003. doi:https://doi.org/10.1088/1748-9326/ac6a6c

He, S., & Xu, Y. J. (2018). Phosphorus fluxes from three coastal watersheds under varied agriculture intensities to the northern gulf of mexico. *Water*, *10*(6), 816. doi:https://doi.org/10.3390/w10060816

House, W. A. (2003). Geochemical cycling of phosphorus in rivers. *Applied Geochemistry, 18*(5), 739-748. Retrieved from https://login.dist.lib.usu.edu/login?url=https://www-proquest-com.dist.lib.usu.edu/docview/19813174?accountid=14761

Ice, G. G., Neary, D. G., & Adams, P. W. (2004). Effects of wildfire on soils and watershed processes. *Journal of Forestry, 102*(6), 16-20. Retrieved from https://login.dist.lib.usu.edu/login?url=https://www.proquest.com/scholarly-journals/effects-wildfire-on-soils-watershed-processes/docview/220831104/se-2?accountid=14761

Johnson, D. W., Walker, R. F., McNulty, M., Rau, B. M., & Miller, W. W. (2012). The long-term effects of wildfire and post-fire vegetation on sierra nevada forest soils. *Forests*, 3(2), 398-416. doi:https://doi.org/10.3390/f3020398

Larson, J. H., James, W. F., Fitzpatrick, F. A., Frost, P. C., Evans, M. A., Reneau, P. C., & Xenopoulos, M. A. (2020). Phosphorus, nitrogen and dissolved organic carbon fluxes from sediments in freshwater river mouths entering green bay (lake michigan; USA). *Biogeochemistry, 147*(2), 179-197. doi:https://doi.org/10.1007/s10533-020-00635-0

Lagerstroem, A., Esberg, C., Wardle, D. A., & Giesler, R. (2009). Soil phosphorus and microbial response to a long-term wildfire chronosequence in northern sweden. *Biogeochemistry*, *95*(2-3), 199-213. doi:https://doi.org/10.1007/s10533-009-9331-y

Lapworth, D. J., Gooddy, D. C., & Jarvie, H. P. (2011). Understanding phosphorus mobility and bioavailability in the hyporheic zone of a chalk stream. *Water, Air and Soil Pollution, 218*(1-4), 213-226. doi:https://doi.org/10.1007/s11270-010-0636-1

Liu, F, Parmenter R, Brooks PD, Conklin MH, Bales RC (2008). Seasonal and interannual variation of streamflow pathways and biogeochemical implications in semi-arid, forested catchments in Valles Caldera, New Mexico. *Ecohydrology, 1*(3):239–252.

Ma, C., Tang, Y., & Ying, J. (2022). Global tectonics and oxygenation events drove the Earth-scale phosphorus cycle. *Earth-Science Reviews*, *233*. https://doi-org/10.1016/j.earscirev.2022.104166

McIntosh, J. C., Schaumberg, C., Perdrial, J., Harpold, A., Angélica Vázquez-Ortega, Rasmussen, C., Chorover, J. (2017). Geochemical evolution of the critical zone across variable time scales informs concentration-discharge relationships: Jemez river basin critical zone observatory. *Water Resources Research*, *53*(5), 4169. doi:https://doi.org/10.1002/2016WR019712

McKenzie, D., Gedalof, Z., Peterson. D.L., and Mote, P. (2004). Climatic change, wildfire, and conservation. *Conservation Biology, 18*, 890-902.

Miesel, J. R., Goebel, P. C., Corace, R. G., Hix, D. M., Kolka, R., Palik, B., & Mladenoff, D. (2012). Fire effects on soils in lake states forests: A compilation of published research to facilitate long-term investigations. *Forests, 3*(4), 1034-1070. doi:https://doi.org/10.3390/f3041034

Miller, W. W., Johnson, D. W., Gergans, N., Carroll-Moore, E., Walker, R. F., Cody, T. L., & Wone, B. (2013). Update on the effects of a sierran wildfire on surface runoff water quality. *Journal of Environmental Quality*, *42*(4), 1185-95. Retrieved from https://login.dist.lib.usu.edu/login?url=https://www.proquest.com/scholarly-journals/update-on-effects-sierran-wildfire-surface-runoff/docview/1420271423/se-2?accountid=14761

Moatar, F., Abbott, B. W., Minaudo, C., Curie, F., and Pinay, G. (2017), Elemental properties, hydrology, and biology interact to shape concentration-discharge curves for carbon, nutrients, sediment, and major ions, *Water Resour. Res.*, *53*, 1270–1287, doi:10.1002/2016WR019635.

National Interagency Coordination Center, Incident Management Situation Report. (9/27/2017). www.nifc.gov/nicc/siterprt.pdf

Noonan, B. J. (2016). *Stream channel erosion as a source of sediment and phosphorous in a central iowa stream* (Order No. 10126563). Available from Agricultural & Environmental Science Collection. (1797608854). Retrieved from https://login.dist.lib.usu.edu/login?url=https://www-proquest-com.dist.lib.usu.edu/dissertations-theses/stream-channel-erosion-as-source-sediment/docview/1797608854/se-2?accountid=14761

Noske, P. J., Lane, P. N. J., & Sheridan, G. J. (2010). Stream exports of coarse matter and phosphorus following wildfire in NE victoria, australia. *Hydrological Processes*, *24*(11), 1514-1529. doi:https://doi.org/10.1002/hyp.7616

Perdrial, J. N., McIntosh, J., Harpold, A., Brooks, P. D., Zapata-Rios, X., Ray, J., Chorover, J. (2014). Stream water carbon controls in seasonally snow-covered mountain catchments: Impact of inter-annual variability of water fluxes, catchment aspect and seasonal processes. *Biogeochemistry*, *118*(1-3), 273-290. doi:https://doi.org/10.1007/s10533-013-9929-y

Prepas, E. E., Burke, J. M., Chanasyk, D. S., Smith, D. W., Putz, G., Gabos, S., . . . Serediak, M. (2003). Impact of wildfire on discharge and phosphorus export from the sakwatamau watershed in the swan hills, alberta, during the first two years. *Journal of Environmental Engineering and Science, 2*, S63-S72. doi:https://doi.org/10.1139/s03-036

Qian, Y., Miao, S. L., Gu, B., & Li, Y. C. (2009). Estimation of postfire nutrient loss in the florida everglades. *Journal of Environmental Quality*, *38*(5), 1812-20. Retrieved from https://login.dist.lib.usu.edu/login?url=https://www.proquest.com/scholarly-

journals/estimation-postfire-nutrient-loss-florida/docview/347858217/se-2?accountid=14761

Rinehart, A.J., Vivoni, E.R., Brooks, P.D. (2008). Effects of vegetation, albedo, and solar radiation sheltering on the distribution of snow in the Valles Caldera, New Mexico. *Ecohydrology*, *1*(3):253–270.

Rust, A. J. (2017). *Wildfire in the west: Evaluating water quality and ecosystem impacts and their controlling factors* (Order No. 10641858). Available from Agricultural & Environmental Science Collection; ProQuest Dissertations & Theses Global. (1994550035). Retrieved from https://login.dist.lib.usu.edu/login?url=https://www.proquest.com/dissertations-theses/wildfire-west-evaluating-water-quality-ecosystem/docview/1994550035/se-2

Sherson, L.R. (2012). Nutrient dynamics in a headwater stream: use of continuous water quality sensors to examine seasonal, event, and diurnal processes in the East Fork Jemez River, NM. M.S. thesis. Department of Earth and Planetary Sciences, University of New Mexico.

Son, J., Kim, S., & Carlson, K. H. (2015). Effects of wildfire on river water quality and riverbed sediment phosphorus. *Water, Air and Soil Pollution*, *226*(3), 1-13. doi:https://doi.org/10.1007/s11270-014-2269-2

Spracklen, D. V., Mickley, L. J., Logan, J. A., Hudman, R. C., Yevich, R., Flannigan, M. D., & Westerling, A. L. (2009). Impacts of climate change from 2000 to 2050 on wildfire activity and carbonaceous aerosol concentrations in the western united states. *Journal of Geophysical Research.D.Atmospheres, 114.* doi:https://doi.org/10.1029/2008JD010966

Verma, S., & Jayakumar, S. (2012). Impact of forest fire on physical, chemical and biological properties of soil: A review. *Proceedings of the International Academy of Ecology and Environmental Sciences, 2*(3), 168. doi:https://doi.org/10.0000/issn-2220-8860-piaees-2012-v2-0018

Wuethrich, C., Schaub, D., Weber, M., Marxer, P., & Conedera, M. (2002). Soil respiration and soil microbial biomass after fire in a sweet chestnut forest in southern switzerland. *Catena, 48*(3), 201-215. doi:https://doi.org/10.1016/S0341-8162(01)00191-6

Xue, L., Li, Q., & Chen, H. (2014). Effects of a wildfire on selected physical, chemical and biochemical soil properties in a pinus massoniana forest in south china. *Forests*, *5*(12), 2947-2966. doi:https://doi.org/10.3390/f5122947

Yan, W., Liu, L., Wu, T., Song, L., Wang, H., Lu, Z. Zhu, Y. (2019). Effects of short-term aerobic conditions on phosphorus mobility in sediments. *Journal of Freshwater Ecology, 34*(1), 649-661. doi:https://doi.org/10.1080/02705060.2019.1659190

Zapata-Rios, X., Troch, P.A., McIntosh, J., Broxton, P., Harpold, A.A., Brooks, P.D. (2012). When winter changes: differences in the hydrological response from first-order catchments of similar age in New Mexico. American Geophysical Union Fall Meeting, San Francisco.

Zhou, A., Tang, H., & Wang, D. (2005). Phosphorus adsorption on natural sediments: Modeling and effects of pH and sediment composition. *Water Research*, *39*(7), 1245–1254. doi:https://doi.org/10.1016/j.watres.2005.01.026

APPENDICES

APPENDIX A

Figure A.1: Storm 1, ISCO 2 hysteresis patterns for SRP (µg·L-1), TP (mg·L^{-1}), and PP (µmols·L^{-1}). Arrows denote overall pattern directionality.

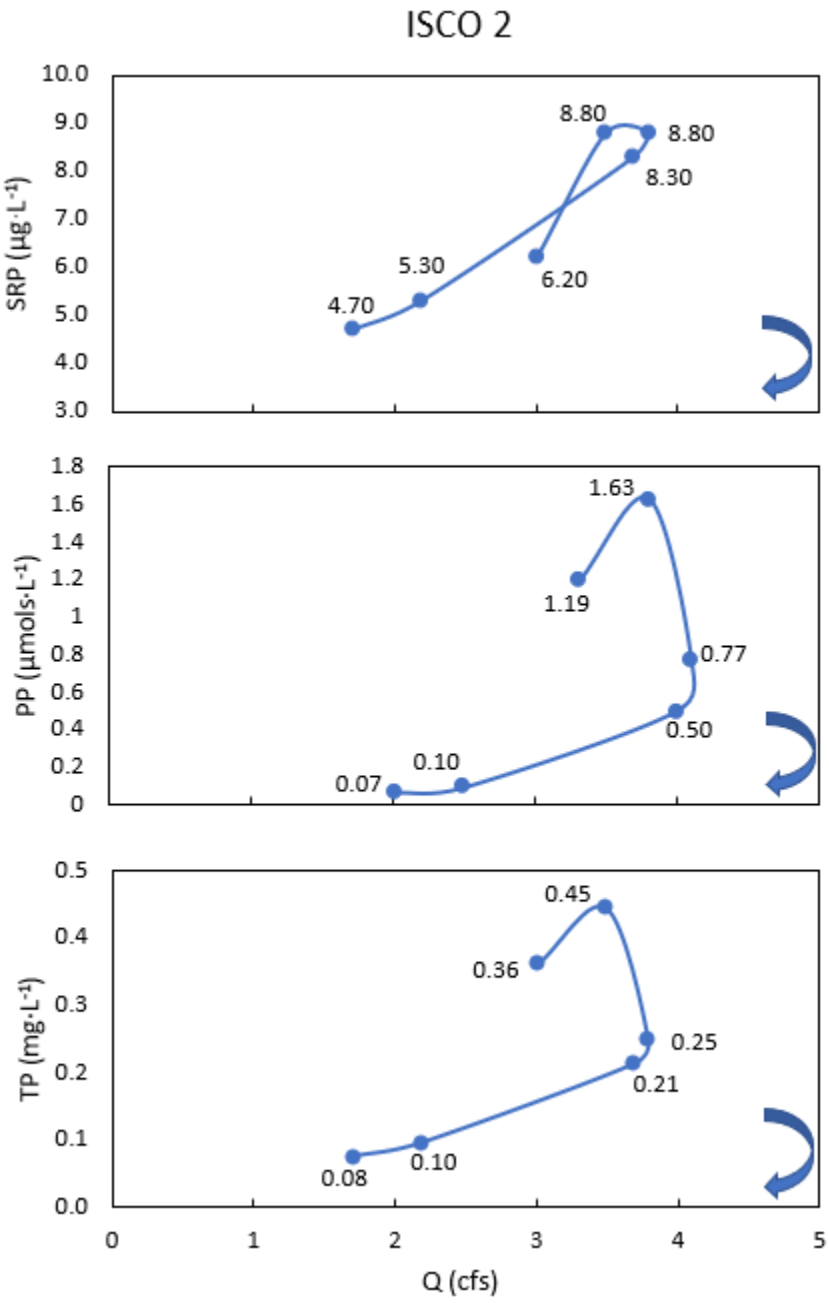

Figure A.1: Storm 1, ISCO 3 hysteresis patterns for SRP (µg·L-1), TP (mg·L^{-1}), and PP (µmols·L^{-1}). Arrows denote overall pattern directionality.

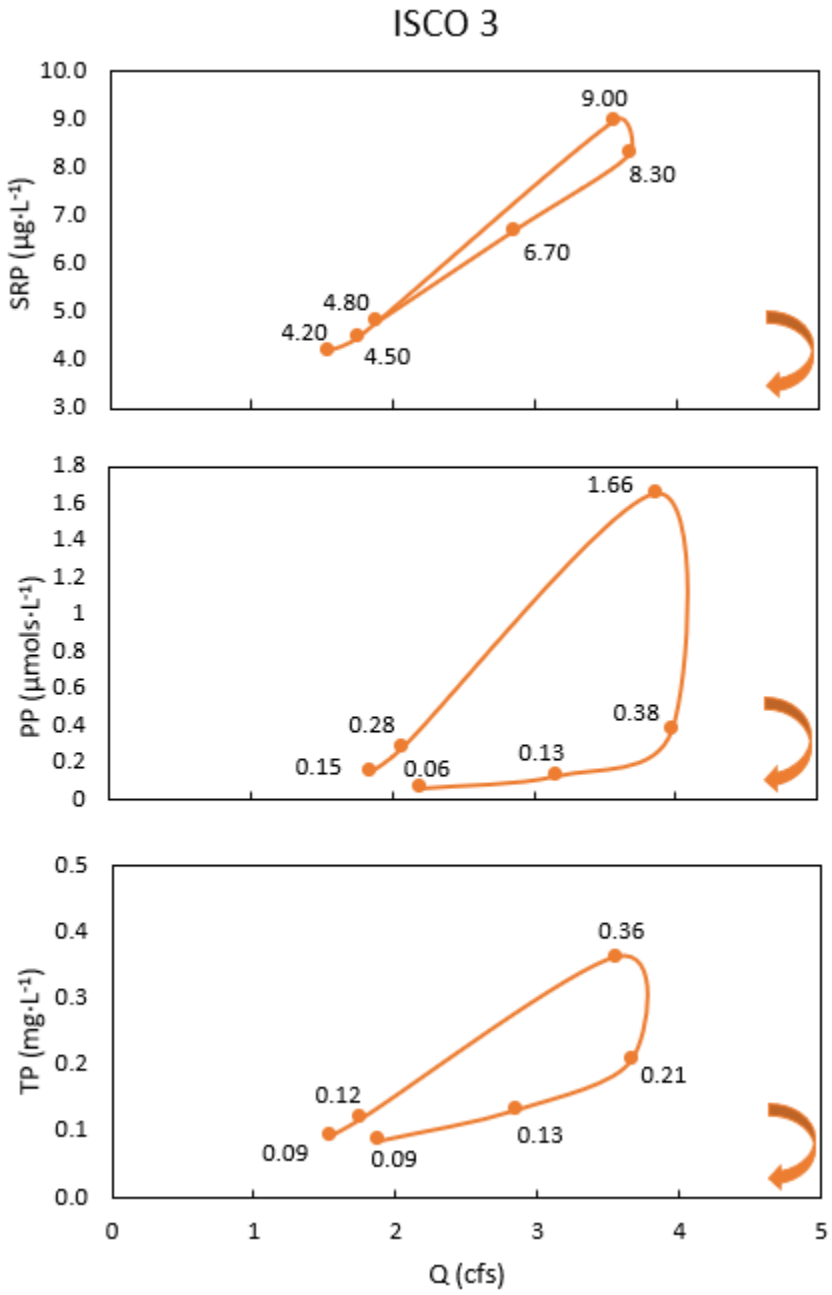

Figure A.2: Storm 2 hysteresis patterns for SRP (µg·L-1), TP (mg·L^{-1}), and PP (µmols·L^{-1}). Arrows denote overall pattern directionality.

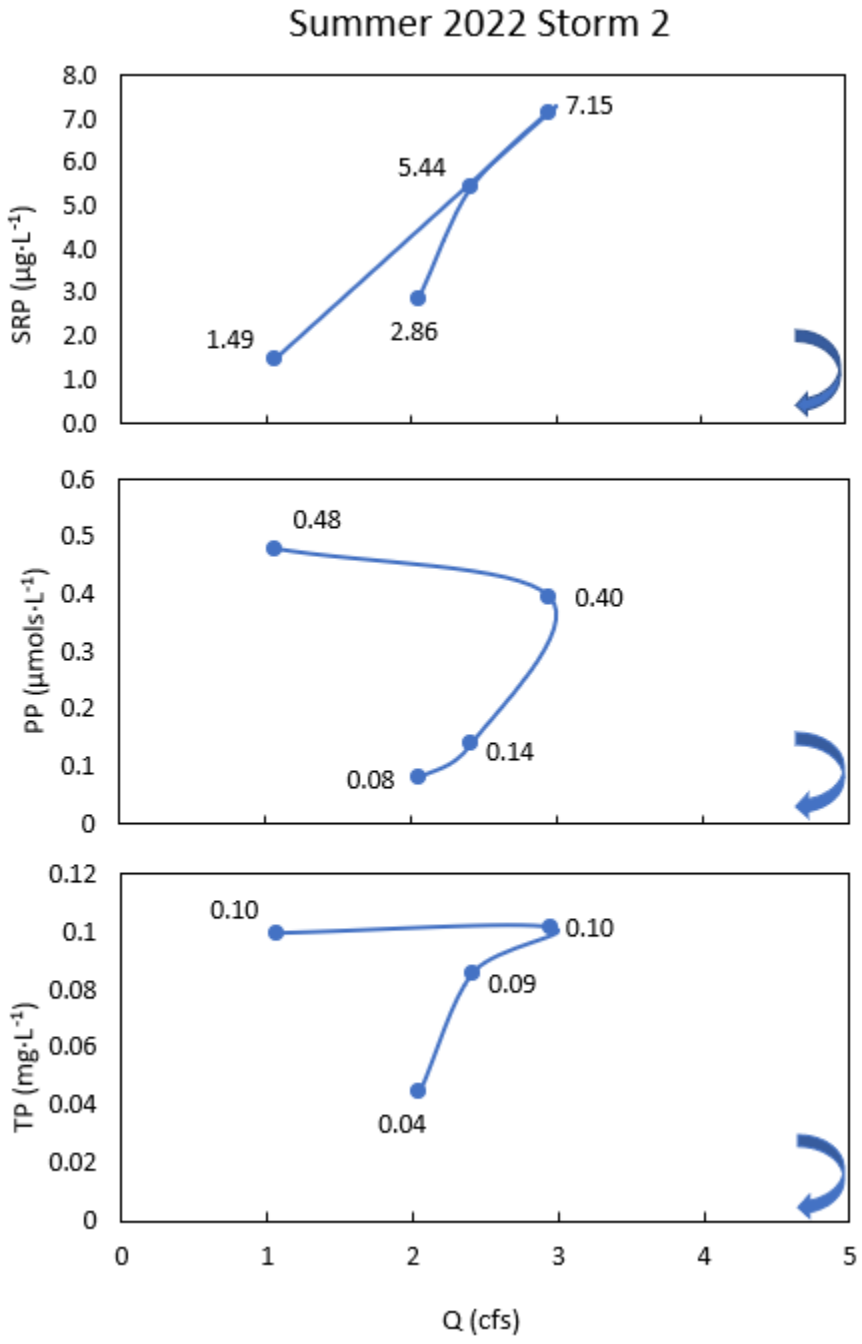

Figure A.3: Storm 3 hysteresis patterns for SRP (µg·L-1), TP (mg·L^{-1}), and PP (µmols·L^{-1}). Arrows denote overall pattern directionality.

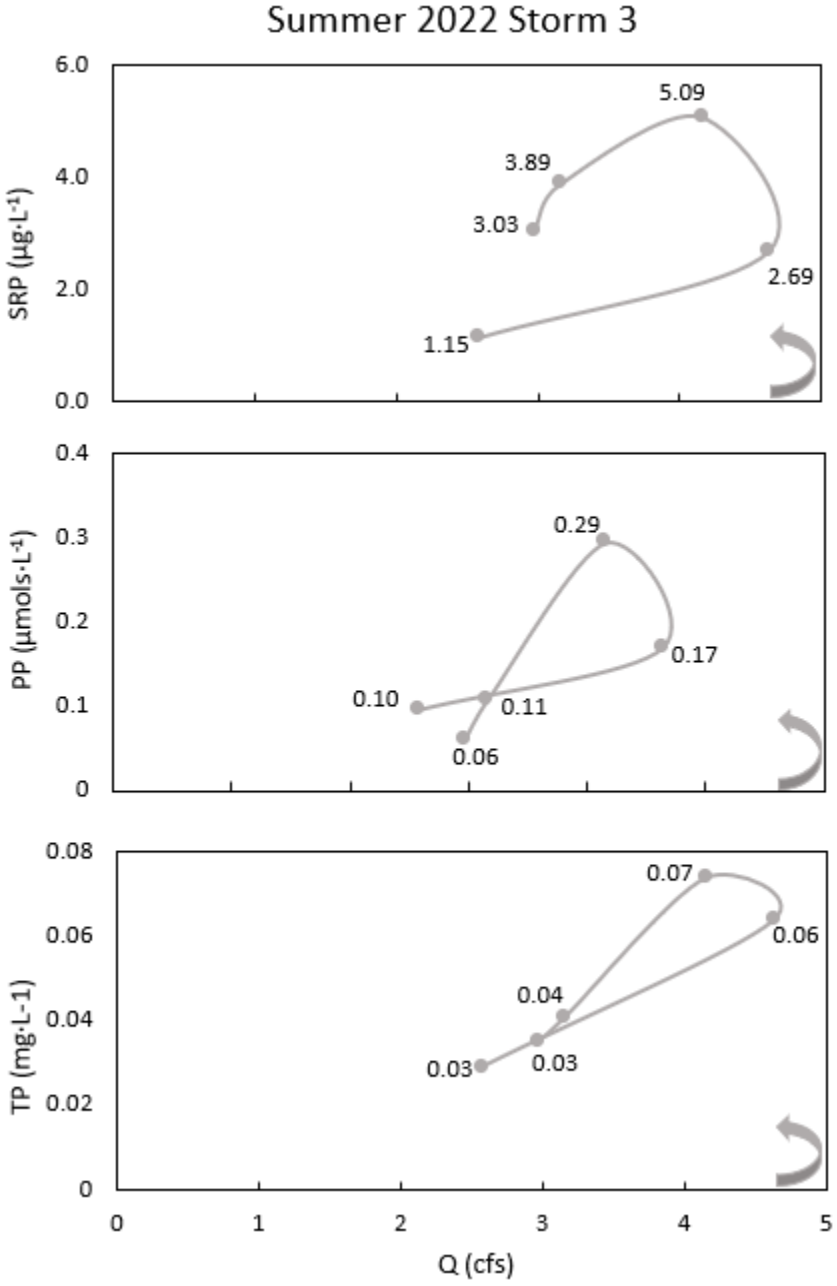

Figure A.4: E1.U hysteresis patterns for SRP (µg·L-1), TP (mg·L^{-1}), and PP (µmols·L^{-1}). Arrows denote overall pattern directionality.

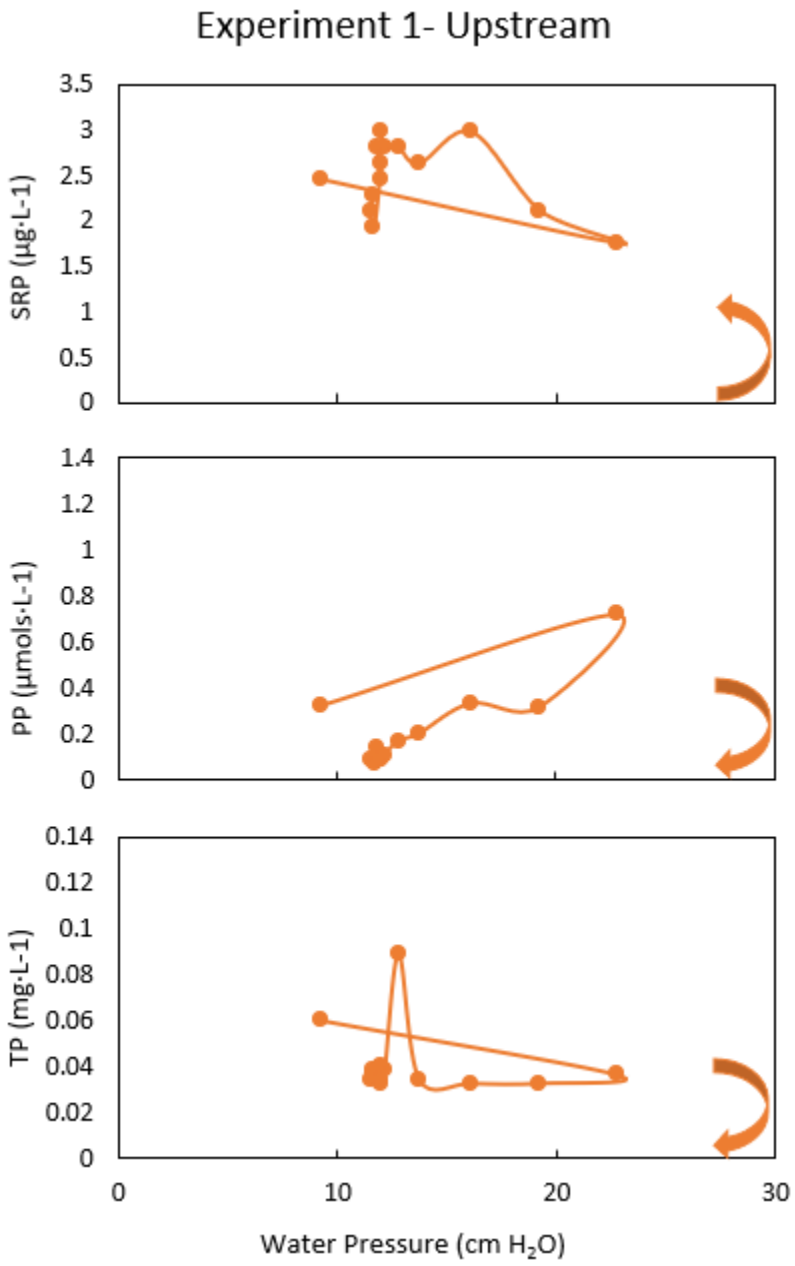

Figure A.5: E1.D hysteresis patterns for SRP (µg·L-1), TP (mg·L^{-1}), and PP (µmols·L^{-1}). Arrows denote overall pattern directionality.

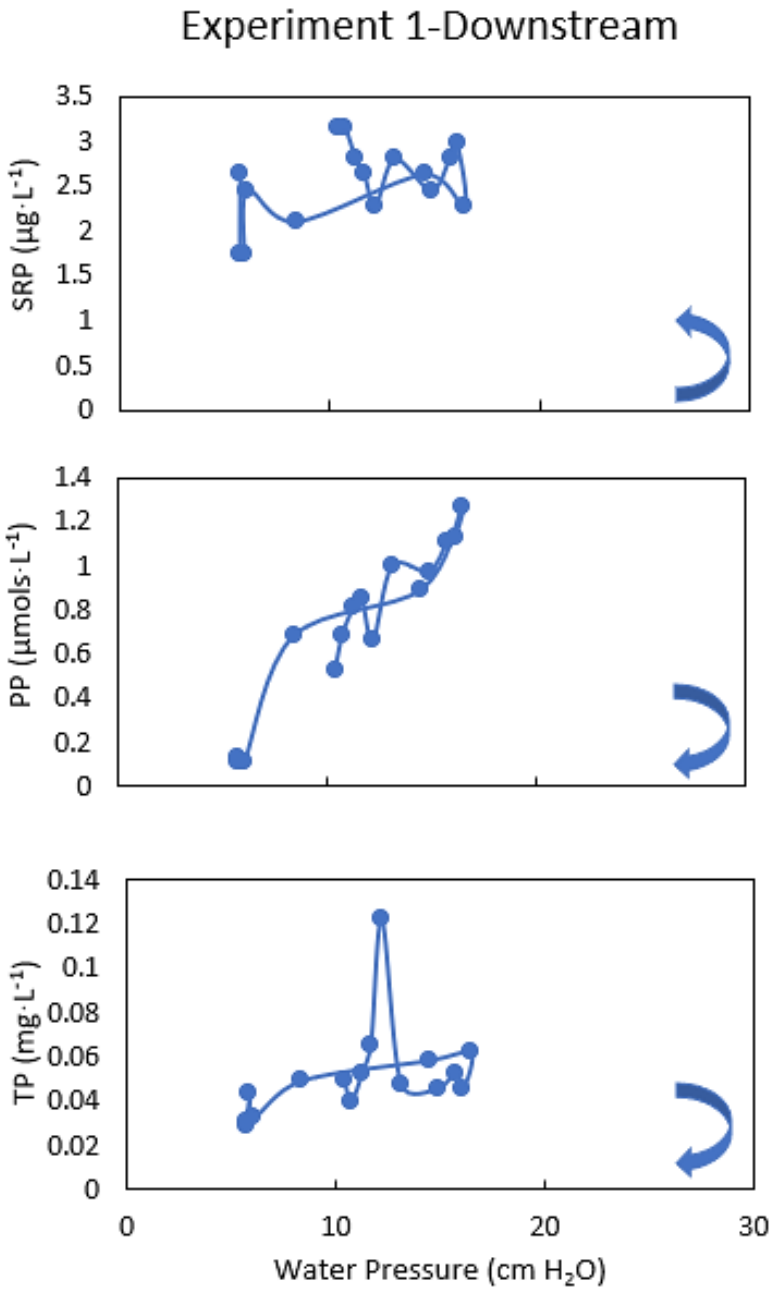

Figure A.6: E5.U hysteresis patterns for SRP (μg·L^{-1}), TP (mg·L^{-1}), and PP (μmols·L^{-1}). Arrows denote overall pattern directionality.

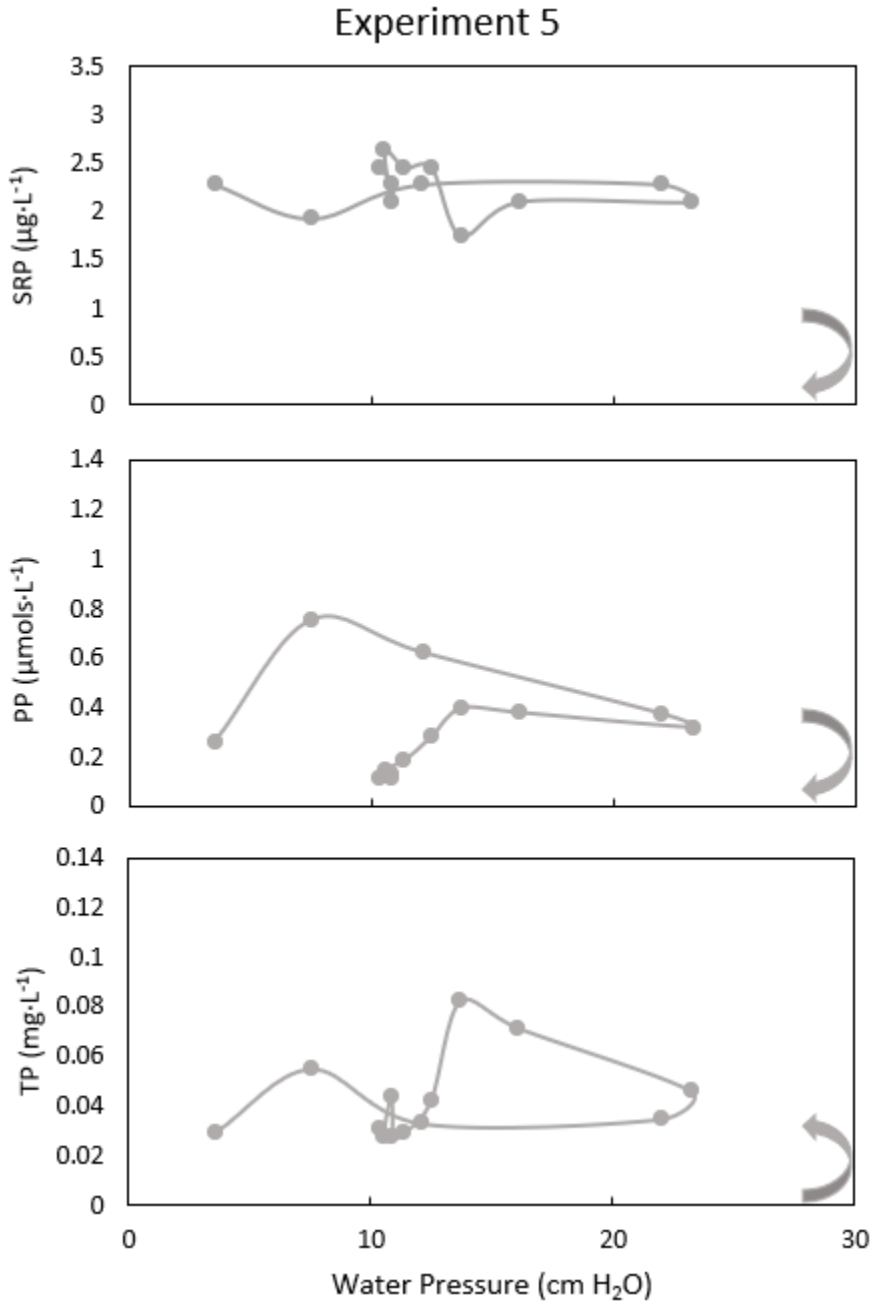

APPENDIX B

Figure B.1: Relationship between watershed attributes and average P (ng) trapped by each DGT in a watershed.

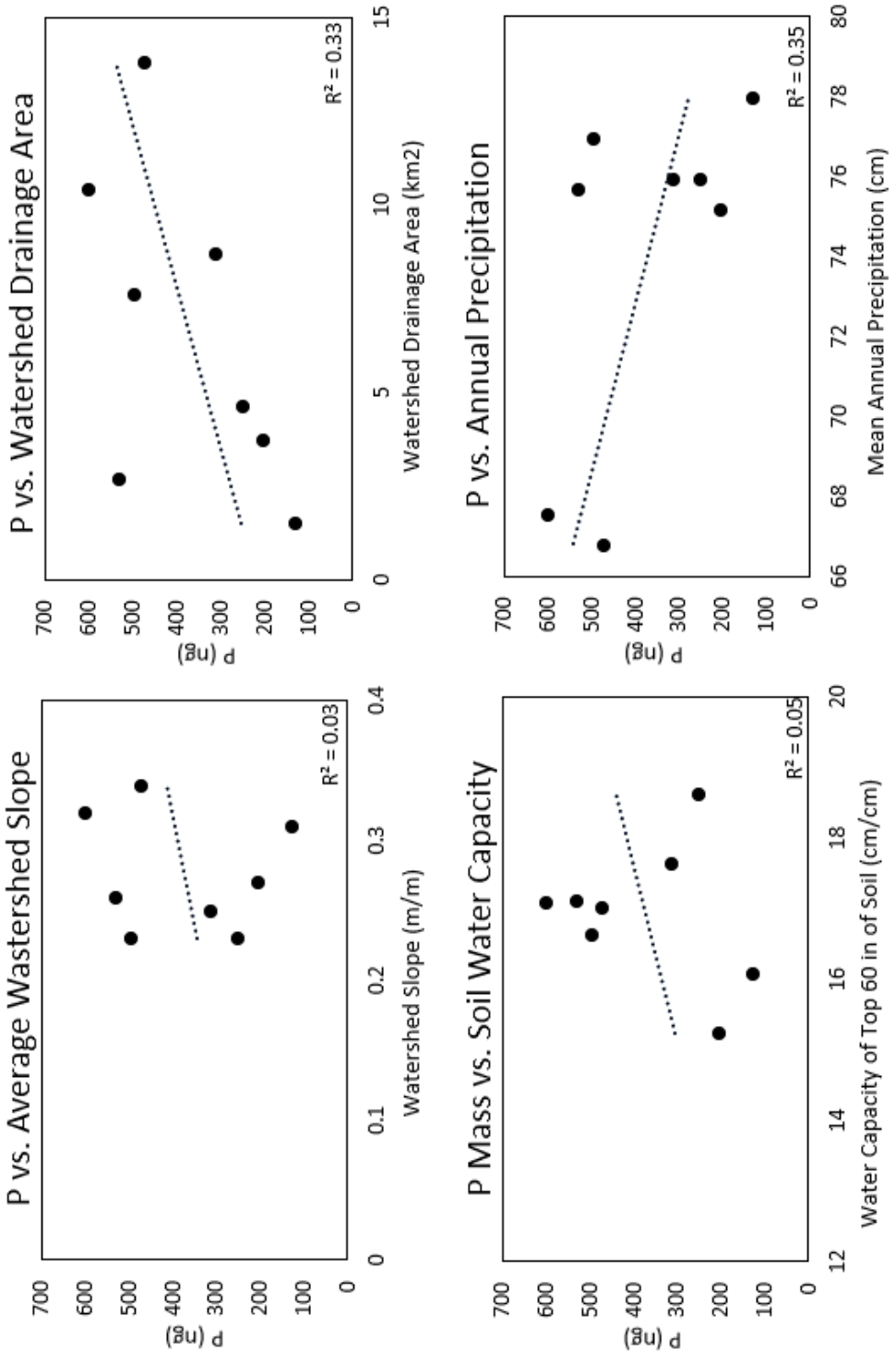

Figure B.2: Relationship between average P (ng) trapped by each DGT in a watershed and vegetation coverage based on type.

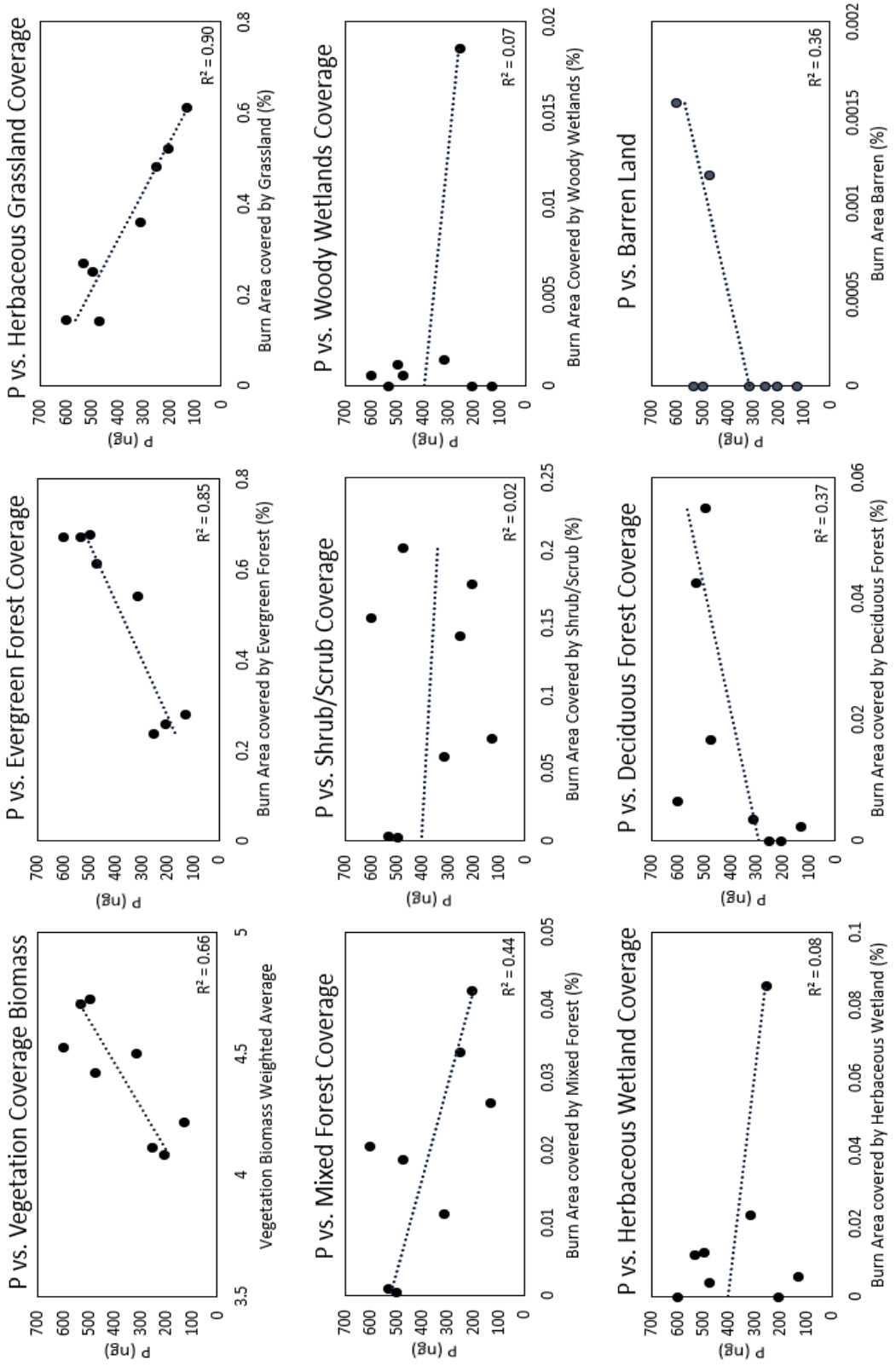

Table B.1: The correlation coefficients and p-values associated with watershed parameter and P mass (ng) accumulated on DGTs. Significance is reported for all obtained p-values, where $^{+}p<0.1$, $^{*}p<0.05$, $^{**}p<0.01$, and $^{***}p<0.001$.

Watershed Parameter	Correlation Coefficient	P-value
Soil Permeability	0.919	0.001***
Vegetation Type	0.795	0.018*
Burn severity	-0.794	0.019*
Elevation ($\bar{x}$)	-0.683	0.062^{+}
Annual Precipitation ($\bar{x}$)	-0.591	0.123
Drainage Area	0.573	0.137
Soil Water Capacity	0.230	0.584
Slope ($\bar{x}$)	0.159	0.708

Table B.2: The correlation coefficients and p-values associated with watershed vegetation coverage and P mass (ng) accumulated on DGTs. Significance is reported for all obtained p-values, where $^{+}p<0.1$, $^{*}p<0.05$, $^{**}p<0.01$, and $^{***}p<0.001$.

Vegetation Type	Correlation Coefficient	P-value
Grassland/Herbaceous	-0.928	0.001***
Evergreen Forest	0.893	0.003**
Deciduous Forest	0.603	0.113
Barren Land	0.603	0.113
Mixed Forest	-0.468	0.242
Herbaceous Wetland	-0.280	0.502
Woody Wetland	-0.242	0.563
Pasture/Hay	0.230	0.583
Shrub/Scrub	-0.140	0.740

Table B.3: Comparison of land area covered by different vegetation types within the experimental watershed's pre-fire (2012) and 6 years post-fire (2019). Green watersheds= unburned, yellow=low, and orange=moderate burn intensities.

Watershed	1		2		3		4		5		6		7		8	
Year	2012	2019	2012	2019	2012	2019	2012	2019	2012	2019	2012	2019	2012	2019	2012	2019
Developed Open Space	0.00	0.00	0.00	0.00	0.01	0.01	0.00	0.00	0.02	0.02	0.00	0.00	0.12	0.12	0.00	0.00
Barren Land	0.00	0.00	0.00	0.00	1.49	0.12	1.77	0.16	0.00	0.00	0.22	0.00	0.17	0.00	0.00	0.00
Deciduous forest	4.26	4.26	5.27	5.46	1.73	1.67	0.86	0.65	0.46	0.36	0.02	0.00	0.02	0.00	1.02	0.23
Evergreen Forest	67.11	67.21	69.83	67.87	84.79	61.39	87.08	67.21	79.07	54.24	74.79	25.88	64.02	23.85	75.13	28.16
Mixed Forest	0.10	0.10	0.06	0.05	2.23	1.87	2.47	2.05	1.61	1.12	9.23	4.19	7.37	3.35	5.27	2.66
Shrub/Scrub	0.30	0.36	0.19	0.26	2.40	20.16	0.88	15.37	0.09	5.79	0.73	17.72	0.58	14.16	0.00	7.03
Grassland/Herbaceous	27.09	26.92	23.41	25.02	6.87	14.31	6.89	14.50	16.62	36.08	15.01	52.20	19.44	48.13	17.96	61.36
Pasture/Hay	0.00	0.00	0.00	0.00	0.03	0.03	0.00	0.00	0.00	0.00	0.00	0.00	0.00	0.00	0.00	0.00
Woody Wetlands	0.00	0.00	0.02	0.12	0.06	0.06	0.06	0.06	0.01	0.15	0.00	0.00	0.00	1.86	0.00	0.00
Emergent Herbaceous Wetlands	1.15	1.15	1.22	1.22	0.39	0.39	0.00	0.00	2.12	2.24	0.00	0.00	8.28	8.53	0.57	0.57
Total Area Covered (%)	100.00	100.00	100.00	100.00	100.00	100.00	100.00	100.00	100.00	100.00	100.00	100.00	100.00	100.00	99.94	100.00